Table 1 Michaelis–Menten kinetic parameters of MDTCS and MDTCS-P475S

	MDTCS	MDTCS-P475S
K_m (μM)	0.37 ± 0.06	0.82 ± 0.12
k_{cat} (s^{-1})	1.94 ± 0.08	1.90 ± 0.11
k_{cat}/K_m (μM^{-1} s^{-1})	5.26 ± 0.52	2.32 ± 0.67
V_{max} (nM s^{-1})	0.35 ± 0.02	0.35 ± 0.02

Values are means ± standard deviation.

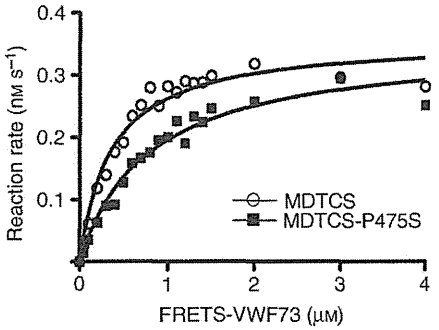

Fig. 2. Kinetic analysis of the cleavage of FRETS-VWF73 by MDTCS and MDTCS-P475S. FRETS-VWF73 (0.05–4 μM) was incubated with MDTCS (open circles, 0.18 nM) or MDTCS-P475S (closed squares, 0.18 nM) at 37 °C. The reaction rate was obtained from the increase in fluorescence over time. The line represents the non-linear fit to the Michaelis–Menten equation. VWF, von Willebrand factor.

When VWF is subjected to shear stress in circulation in vivo or denaturants in vitro, the A2 domain unfolds and adopts a partially extended conformation that makes its scissile peptide bond accessible for cleavage by ADAMTS-13 [19,35]. VWF treated with mechanistic-induced flow on a vortex mixer can be easily cleaved by ADAMTS-13 [30], so this fluid shear-treated VWF-cleaving assay is useful for the investigation of ADAMTS-13 function and regulation. We examined the activities of MDTCS and MDTCS-P475S against shear-treated VWF. VWF cleavage was monitored by the appearance of the 150-kDa band on western blotting with the anti-VWF antibody. Although both MDTCS and MDTCS-P475S produced the 150-kDa fragment band after a 10-min incubation, the band intensity was weaker for MDTCS-P475S (63% ± 8.2% at 120 min) than for MDTCS (Fig. 3A). Shearing treatment of MDTCS-P475S did not affect VWF-cleaving activity (Fig. 3B). These results suggest that MDTCS-P475S moderately cleaves VWF, once the scissile bond in VWF is exposed by shear stress. Shear treatment-induced cleavage of VWF by MDTCS-P475S was more severely inhibited than that by MDTCS upon the addition of urea. The VWF-cleaving activities of MDTCS and MDTCS-P475S in the presence of 1.5 M urea were 47.0% ± 6.5% and 8.9% ± 1.9%, respectively (Fig. 3C).

Effects of denaturants and temperature on the enzymatic activities of MDTCS and MDTCS-P475S

As the addition of urea severely inhibited the shear-dependent cleavage of VWF by MDTCS-P475S, we examined the effects of denaturants on the activity of MDTCS and MDTCS-P475S by using FRETS-VWF73. The reaction rates of MDTCS and MDTCS-P475S were

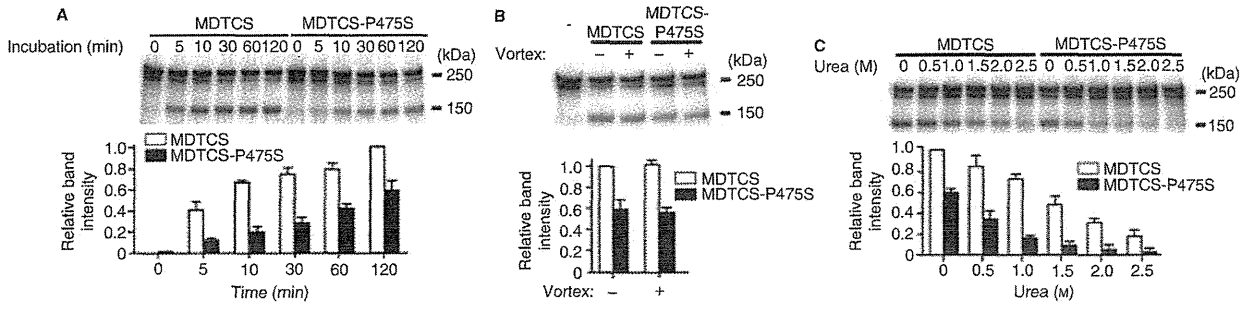

Fig. 3. Cleavage of shear-treated von Willebrand factor (VWF) by MDTCS and MDTCS-P475S. (A) Top: western blotting image showing VWF cleavage at each time point. The VWF multimer (25 μg mL^{-1}; 100 nM VWF monomers) was treated with shear with a 3-min vortex at 2500 r.p.m. at 24 °C, and MDTCS or MDTCS-P475S (1 nM) was then added to the reaction mixture. After incubation for the indicated times (0–120 min) at 37 °C, VWF cleavage was detected by the appearance of the 150-kDa band on western blotting with the anti-VWF antibody. Bottom: densitometric analysis of VWF cleavage. The band intensities of the cleavage products (150 kDa) were quantified as described in Materials and Methods. Band intensities relative to that of MDTCS at 120 min (set as 1) were plotted as means ± standard deviation (n = 3). (B) Top: western blotting image showing VWF cleavage by shear-treated or untreated MDTCS or MDTCS-P475S. The VWF multimer (25 μg mL^{-1}) was treated by shearing with vortexing for 3 min, and MDTCS or MDTCS-P475S (1 nM each), treated with shearing (2500 r.p.m. for 10 min), was then added to the reaction mixture. After incubation for 120 min at 37 °C, the cleavage of shear-treated VWF was detected as described in (A). Bottom: densitometric analysis of VWF cleavage. Band intensities relative to that of MDTCS without vortex (set as 1) were plotted as means ± standard deviation (n = 3). (C) Top: western blotting image showing VWF cleavage at various concentrations of urea. The VWF multimer (25 μg mL^{-1}) was treated with shear with a 3-min vortex, and MDTCS or MDTCS-P475S (1 nM each) was then added to the reaction mixture containing 0–2.5 M urea. After incubation for 120 min at 37 °C, the cleavage of shear-treated VWF was detected as described in (A). Bottom: densitometric analysis of VWF cleavage. Band intensities relative to that of MDTCS at 0 M urea (set as 1) were plotted as means ± standard deviation (n = 3).

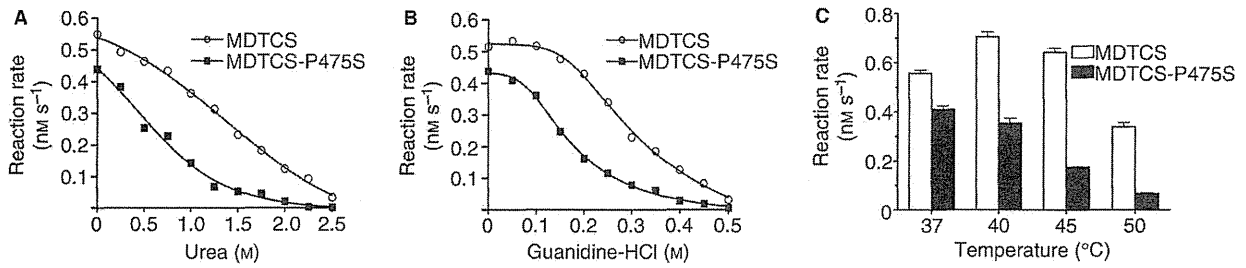

Fig. 4. Effects of denaturants and temperature on the FRETS-VWF73-cleaving activity of MDTCS and MDTCS-P475S. The enzymatic activities of MDTCS and MDTCS-P475S (0.8 nM) were measured for 60 min by the use of FRETS-VWF73 (1 μM) in the presence of urea (A) or guanidine-HCl (B) at 37 °C, or at different reaction temperatures (C). Values are means ± standard deviation (C: $n = 3$). VWF, von Willebrand factor.

reduced according to the concentrations of urea (Fig. 4A) or guanidine-HCl (Fig. 4B). The half-maximal inhibitory concentration (IC_{50}) for urea was 1.5 M for MDTCS and 0.8 M for MDTCS-P475S. The IC_{50} for guanidine-HCl was 0.3 M for MDTCS and 0.15 M for MDTCS-P475S. Furthermore, the activities of MDTCS and MDTCS-P475S were measured at 37, 40, 45 and 50 °C (Fig. 4C). A higher reaction temperature caused a more severe decrease in the activity of MDTCS-P475S than of MDTCS.

Discussion

Racial or ethnic group-specific genetic factors are now recognized to be important factors in the pathogenesis of thrombosis [36,37]. We previously identified the dysfunctional P475S polymorphism in ADAMTS-13 [8], and showed that it is East Asian-specific [14]. In the present study, we demonstrated that MDTCS-P475S showed moderate cleavage activity against shear-treated VWF, suggesting that the P475S polymorphism is not a causative factor in the development of TTP. However, this does not exclude the possibility that the P475S polymorphism could increase the risk for acquired TTP caused by inhibitory autoantibodies against ADAMTS-13. The relationship of the P475S polymorphism with acquired TTP remains to be addressed.

Recent studies have indicated the important function of the D and S domains as substrate-binding exosites [19–21]. We have identified at least three putative VWF-binding exosites, within the D, C_A and S domains, linearly aligned in the three-dimensional structure [18]. In the present study, kinetic analysis with FRETS-VWF73 showed that the lower catalytic efficiency (k_{cat}/K_m) of MDTCS-P475S was caused by lower affinity (higher K_m) but not by lower catalytic activity (lower k_{cat}). This also supports the idea that the V-loop in the C_A domain is a VWF-binding exosite.

The thermal shift assay showed that the thermostabilities of MDTCS and MDTCS-P475S were almost the same. Although the interaction between Ser475 in the V-loop of the C_A domain and Leu620 in the β6–β7 loop of the S domain was disrupted in the MDTCS-P475S structure, van der Waals contacts between Leu621 in the S domain and a hydrophobic pocket in the C_A domain formed by Gln442, Leu443, Met446, Val474, Arg507, Cys508 and Met509 [18] were retained. These interactions may minimize the adverse effect of P475S substitution on the stability of the S domain. These observations suggest that the reduction in the activity of MDTCS-P475S is not a consequence of global protein instability, but rather of a reduction in the enzyme–substrate interaction owing to the local conformational change in the V-loop (especially interatomic interactions with Ser475) (Fig. 1D). The greatly reduced enzymatic activity of MDTCS-P475S in the presence of urea and at a higher reaction temperature suggests that the P475S substitution induces a more severe local conformational change in the V-loop under these conditions and reduces the enzyme–substrate interaction.

Pro475 is conserved in all primates examined but not in other species (Fig. S3). Mouse ADAMTS-13 shows significantly reduced enzymatic activity against human VWF [38], indicating the species specificity of the ADAMTS-13–VWF interaction. Several amino acids in the core binding region for ADAMTS-13 in the A2 domain of VWF (VWF73) [39] differ among species (Fig. S4). Non-conserved amino acids in the exosites of ADAMTS-13 and in the VWF73 region of VWF may have coevolved for species-specific ADAMTS-13–VWF interface recognition.

Post-translational protein *C*-mannosylation is the attachment of an α-mannopyranosyl residue to the indole C-2 of tryptophan via a C–C linkage [32]. Proteins known to be *C*-mannosylated are RNase, interleukin-12, the mucins MUC5AC and MUC5B, and several proteins containing TSRs, such as thrombospondin-1, F-spondin, C6, C7, properdin, ADAMTS-L1, and ADAMTS-5 [33]. In the present study, potential *C*-mannosylation of Trp387 in the T1 domain of ADAMTS-13 has been suggested for the first time. *C*-mannosylation typically occurs in TSRs within the sequence motif W*XX*W, which is highly conserved among ADAMTS family members (ADAMTSs and ADAMTS-Ls) [33]. The functional role of *C*-mannosylation in ADAMTS-13 is unknown; however, a *C*-

mannosylation defect in ADAMTS-L1 decreases its secretion, suggesting a role in the regulation of protein secretion [33].

Addendum

M. Akiyama, D. Nakayama, and S. Takeda: performed research, analyzed data, and wrote the manuscript; K. Kokame: designed the experiments; J. Takagi: provided laboratory reagents; T. Miyata: wrote the manuscript and provided funding. All authors have approved the final draft.

Acknowledgements

The authors thank Y. Fujimura at Nara Medical University for providing us with purified plasma VWF. We also thank T. Kunieda for her help with protein purification, and M. Tomisako for her help with crystallization. This work was supported by grants-in-aid from the Ministry of Health, Labor, Welfare of Japan, the Ministry of Education, Culture, Sports, Science and Technology of Japan, and the SENSHIN Medical Research Foundation.

Disclosure of Conflict of Interests

The authors state that they have no conflict of interest.

Supporting Information

Additional Supporting Information may be found in the online version of this article:

Figure S1. Calibration curves for FRETS-VWF73 cleavage.
Figure S2. Thermal shift assay profiles of MDTCS and MDTCS-P475S.
Figure S3. Amino acid sequence alignment of the C_A domain of ADAMTS-13 from different species.
Figure S4. Amino acid sequence alignment of the core binding region for ADAMTS-13 in the A2 domain of VWF from different species.
Table S1. Data collection and refinement statistics.

References

1 Springer TA. Biology and physics of von Willebrand factor concatamers. *J Thromb Haemost* 2011; **9**(Suppl. 1): 130–43.
2 Dent JA, Galbusera M, Ruggeri ZM. Heterogeneity of plasma von Willebrand factor multimers resulting from proteolysis of the constituent subunit. *J Clin Invest* 1991; **88**: 774–82.
3 Tsai HM, Sussman II, Nagel RL. Shear stress enhances the proteolysis of von Willebrand factor in normal plasma. *Blood* 1994; **83**: 2171–9.
4 Sadler JE, Moake JL, Miyata T, George JN. Recent advances in thrombotic thrombocytopenic purpura. *Hematology Am Soc Hematol Educ Program* 2004; **2004**: 407–23.
5 Soejima K, Mimura N, Hirashima M, Maeda H, Hamamoto T, Nakagaki T, Nozaki C. A novel human metalloprotease synthesized in the liver and secreted into the blood: possibly, the von Willebrand factor-cleaving protease? *J Biochem* 2001; **130**: 475–80.
6 Levy GG, Nichols WC, Lian EC, Foroud T, McClintick JN, McGee BM, Yang AY, Siemieniak DR, Stark KR, Gruppo R, Sarode R, Shurin SB, Chandrasekaran V, Stabler SP, Sabio H, Bouhassira EE, Upshaw JD Jr, Ginsburg D, Tsai HM. Mutations in a member of the ADAMTS gene family cause thrombotic thrombocytopenic purpura. *Nature* 2001; **413**: 488–94.
7 Zheng X, Chung D, Takayama TK, Majerus EM, Sadler JE, Fujikawa K. Structure of von Willebrand factor-cleaving protease (ADAMTS13), a metalloprotease involved in thrombotic thrombocytopenic purpura. *J Biol Chem* 2001; **276**: 41059–63.
8 Kokame K, Matsumoto M, Soejima K, Yagi H, Ishizashi H, Funato M, Tamai H, Konno M, Kamide K, Kawano Y, Miyata T, Fujimura Y. Mutations and common polymorphisms in ADAMTS13 gene responsible for von Willebrand factor-cleaving protease activity. *Proc Natl Acad Sci USA* 2002; **99**: 11902–7.
9 Lotta LA, Garagiola I, Palla R, Cairo A, Peyvandi F. ADAMTS13 mutations and polymorphisms in congenital thrombotic thrombocytopenic purpura. *Hum Mutat* 2010; **31**: 11–19.
10 Kokame K, Kokubo Y, Miyata T. Polymorphisms and mutations of ADAMTS13 in the Japanese population and estimation of the number of patients with Upshaw–Schulman syndrome. *J Thromb Haemost* 2011; **9**: 1654–6.
11 Jang MJ, Kim NK, Chong SY, Kim HJ, Lee SJ, Kang MS, Oh D. Frequency of Pro475Ser polymorphism of ADAMTS13 gene and its association with ADAMTS-13 activity in the Korean population. *Yonsei Med J* 2008; **49**: 405–8.
12 Gao W, Ruan C, Dai L, Su J, Wang Z. The frequency of P475S polymorphism in von Willebrand factor-cleaving protease in the Chinese population and its relevance to arterial thrombotic disorders. *Thromb Haemost* 2004; **91**: 1257–8.
13 Bongers TN, De Maat MP, Dippel DW, Uitterlinden AG, Leebeek FW. Absence of Pro475Ser polymorphism in ADAMTS-13 in Caucasians. *J Thromb Haemost* 2005; **3**: 805.
14 Kokame K, Miyata T. Genetic defects leading to hereditary thrombotic thrombocytopenic purpura. *Semin Hematol* 2004; **41**: 34–40.
15 Akiyama M, Kokame K, Miyata T. ADAMTS13 P475S polymorphism causes a lowered enzymatic activity and urea lability *in vitro*. *J Thromb Haemost* 2008; **6**: 1830–2.
16 Soejima K, Matsumoto M, Kokame K, Yagi H, Ishizashi H, Maeda H, Nozaki C, Miyata T, Fujimura Y, Nakagaki T. ADAMTS-13 cysteine-rich/spacer domains are functionally essential for von Willebrand factor cleavage. *Blood* 2003; **102**: 3232–7.
17 Zheng X, Nishio K, Majerus EM, Sadler JE. Cleavage of von Willebrand factor requires the spacer domain of the metalloprotease ADAMTS13. *J Biol Chem* 2003; **278**: 30136–41.
18 Akiyama M, Takeda S, Kokame K, Takagi J, Miyata T. Crystal structures of the noncatalytic domains of ADAMTS13 reveal multiple discontinuous exosites for von Willebrand factor. *Proc Natl Acad Sci USA* 2009; **106**: 19274–9.
19 Crawley JT, de Groot R, Xiang Y, Luken BM, Lane DA. Unraveling the scissile bond: how ADAMTS13 recognizes and cleaves von Willebrand factor. *Blood* 2011; **118**: 3212–21.
20 Wu JJ, Fujikawa K, McMullen BA, Chung DW. Characterization of a core binding site for ADAMTS-13 in the A2 domain of von Willebrand factor. *Proc Natl Acad Sci USA* 2006; **103**: 18470–4.
21 Jin SY, Skipwith CG, Zheng XL. Amino acid residues Arg(659), Arg(660), and Tyr(661) in the spacer domain of ADAMTS13 are critical for cleavage of von Willebrand factor. *Blood* 2010; **115**: 2300–10.

22 Pos W, Crawley JT, Fijnheer R, Voorberg J, Lane DA, Luken BM. An autoantibody epitope comprising residues R660, Y661, and Y665 in the ADAMTS13 spacer domain identifies a binding site for the A2 domain of VWF. *Blood* 2010; **115**: 1640–9.
23 Akiyama M, Takeda S, Kokame K, Takagi J, Miyata T. Production, crystallization and preliminary crystallographic analysis of an exosite-containing fragment of human von Willebrand factor-cleaving proteinase ADAMTS13. *Acta Crystallogr F Struct Biol Crystallogr Commun* 2009; **65**: 739–42.
24 Reeves PJ, Callewaert N, Contreras R, Khorana HG. Structure and function in rhodopsin: high-level expression of rhodopsin with restricted and homogeneous *N*-glycosylation by a tetracycline-inducible *N*-acetylglucosaminyltransferase I-negative HEK293S stable mammalian cell line. *Proc Natl Acad Sci USA* 2002; **99**: 13419–24.
25 Winn MD, Ballard CC, Cowtan KD, Dodson EJ, Emsley P, Evans PR, Keegan RM, Krissinel EB, Leslie AG, McCoy A, McNicholas SJ, Murshudov GN, Pannu NS, Potterton EA, Powell HR, Read RJ, Vagin A, Wilson KS. Overview of the CCP4 suite and current developments. *Acta Crystallogr D Biol Crystallogr* 2011; **67**: 235–42.
26 Emsley P, Lohkamp B, Scott WG, Cowtan K. Features and development of Coot. *Acta Crystallogr D Biol Crystallogr* 2010; **66**: 486–501.
27 Brunger AT. Version 1.2 of the crystallography and NMR system. *Nat Protoc* 2007; **2**: 2728–33.
28 Kokame K, Nobe Y, Kokubo Y, Okayama A, Miyata T. FRETS-VWF73, a first fluorogenic substrate for ADAMTS13 assay. *Br J Haematol* 2005; **129**: 93–100.
29 Anderson PJ, Kokame K, Sadler JE. Zinc and calcium ions cooperatively modulate ADAMTS13 activity. *J Biol Chem* 2006; **281**: 850–7.
30 Zhang P, Pan W, Rux AH, Sachais BS, Zheng XL. The cooperative activity between the carboxyl-terminal TSP1 repeats and the CUB domains of ADAMTS13 is crucial for recognition of von Willebrand factor under flow. *Blood* 2007; **110**: 1887–94.
31 De Marco L, Shapiro SS. Properties of human asialo-factor VIII. A ristocetin-independent platelet-aggregating agent. *J Clin Invest* 1981; **68**: 321–8.
32 Gonzalez de Peredo A, Klein D, Macek B, Hess D, Peter-Katalinic J, Hofsteenge J. *C*-mannosylation and *O*-fucosylation of thrombospondin type 1 repeats. *Mol Cell Proteomics* 2002; **1**: 11–18.
33 Wang LW, Leonhard-Melief C, Haltiwanger RS, Apte SS. Post-translational modification of thrombospondin type-1 repeats in ADAMTS-like 1/punctin-1 by *C*-mannosylation of tryptophan. *J Biol Chem* 2009; **284**: 30004–15.
34 Zhang Q, Zhou YF, Zhang CZ, Zhang X, Lu C, Springer TA. Structural specializations of A2, a force-sensing domain in the ultralarge vascular protein von Willebrand factor. *Proc Natl Acad Sci USA* 2009; **106**: 9226–31.
35 Zhang X, Halvorsen K, Zhang CZ, Wong WP, Springer TA. Mechanoenzymatic cleavage of the ultralarge vascular protein von Willebrand factor. *Science* 2009; **324**: 1330–4.
36 Zakai NA, McClure LA. Racial differences in venous thromboembolism. *J Thromb Haemost* 2011; **9**: 1877–82.
37 Miyata T, Hamasaki N, Wada H, Kojima T. More on: racial differences in venous thromboembolism. *J Thromb Haemost* 2012; **10**: 319–20.
38 Zhou W, Bouhassira EE, Tsai HM. An IAP retrotransposon in the mouse ADAMTS13 gene creates ADAMTS13 variant proteins that are less effective in cleaving von Willebrand factor multimers. *Blood* 2007; **110**: 886–93.
39 Kokame K, Matsumoto M, Fujimura Y, Miyata T. VWF73, a region from D1596 to R1668 of von Willebrand factor, provides a minimal substrate for ADAMTS-13. *Blood* 2004; **103**: 607–12.

Mise et al. BMC Nephrology 2013, 14:156
http://www.biomedcentral.com/1471-2369/14/156

BMC Nephrology

CASE REPORT Open Access

Long term follow up of congenital thrombotic thrombocytopenic purpura (Upshaw-Schulman syndrome) on hemodialysis for 19 years: a case report

Koki Mise[1,6*], Yoshifumi Ubara[1,3,6], Masanori Matsumoto[4], Keiichi Sumida[1,6], Rikako Hiramatsu[1], Eiko Hasegawa[1], Masayuki Yamanouchi[1], Noriko Hayami[1,6], Tatsuya Suwabe[1,6], Junichi Hoshino[1,6], Naoki Sawa[1], Kenichi Ohashi[2], Koichi Kokame[5], Toshiyuki Miyata[5], Yoshihiro Fujimura[4] and Kenmei Takaichi[1,3]

Abstract

Background: Thrombotic thrombocytopenic purpura (TTP) is frequently associated with renal abnormalities, but there have been few reports about renal abnormalities in patients with hereditary TTP. In particular, little is known about the long-term prognosis of patients with childhood-onset congenital TTP.

Case presentation: We report a Japanese patient with congenital TTP (Upshaw–Schulman syndrome) who was followed for 19 years after initiation of hemodialysis when he was 22 years old. At the age of 6 years, the first episode of purpura, thrombocytopenia, and proteinuria occurred without any precipitating cause. He underwent living-related donor kidney transplantation from his mother, but the graft failed after 5 months due to recurrence of TTP. Even after resection of the transplanted kidney and resumption of regular hemodialysis, TTP became refractory to infusion of fresh frozen plasma (FFP). Therefore, splenectomy was performed and his disease remained in remission for 10 years. However, TTP recurred at the age of 39 years. Plasma activity of ADAMTS13 (a disintegrin and metalloprotease with thrombospondin type I domain 13) was less than 3%, while ADAMTS13 inhibitor was not detected (< 0.5 Bethesda units/mL). The patient died suddenly after hemodialysis at the age of 41 years. Subsequent genetic analysis of this patient and his parents revealed two different heterozygous mutations of ADAMTS13, including a missense mutation in exon 26 (c.3650T>C causing p.I1217T) inherited from his father and a missense mutation in exon 21 (c.2723G>A causing p.C908Y) inherited from his mother. The former mutation has not been detected before in Japan, while the latter mutation is common in Japan. A retrospective review showed that serum C3 levels were consistently low while C4 levels were normal during follow-up, and C3 decreased much further during each episode of TTP.

Conclusion: Congenital TTP was diagnosed from the clinical, biochemical, and genetic findings. Infusion of FFP controlled each thrombotic episode, but the effect was limited and of short duration. Review of the complement profile in this patient suggested that a persistently low serum C3 level might be associated with refractory TTP and a worse renal prognosis.

Keywords: Congenital thrombotic thrombocytopenic purpura, ADAMTS13 (a disintegrin and metalloprotease with thrombospondin type I domain 13), Chronic hemodialysis, Complement activation, C3, Alternative pathway

* Correspondence: kokims-frz@umin.ac.jp
[1]Nephrology Center, Toranomon Hospital, Tokyo, Japan
[6]Nephrology Center, Toranomon Hospital Kajigaya, 1-3-1, Kajigaya, Takatu-ku, Kawasaki-shi, Kanagawa-ken 213-0015, Japan
Full list of author information is available at the end of the article

Background

Thrombotic thrombocytopenic purpura (TTP) is a rare disorder characterized by thrombocytopenia and microangiopathic hemolytic anemia. Congenital TTP has been reported to be associated with severe deficiency of the plasma activity of ADAMTS13 (a disintegrin and metalloprotease with thrombospondin type I domain 13), which is reduced to <5% of normal by mutation of the ADAMTS13 gene, and this is known as the Upshaw–Schulman syndrome (USS) [1,2]. Deficiency of ADAMTS13 activity can also be caused by inhibitory antibodies targeting ADAMTS13, leading to acquired TTP. ADAMTS13 is a metalloproteinase that specifically cleaves multimeric von Willebrand factor (VWF) [2], while VWF is a large glycoprotein that is essential for platelet adhesion and aggregation under high shear stress conditions [3]. ADAMTS13 is mainly synthesized in the liver by stellate cells [4,5]. In addition, it is expressed by the podocytes and endothelium of the renal glomeruli, where podocyte-derived ADAMTS13 might have a local protective effect in the high shear stress glomerular microcirculation [6].

TTP is often associated with renal abnormalities and there have been some reports about such abnormalities in TTP patients, but few about hereditary TTP. In particular, there is little information about the long-term prognosis of patients with childhood-onset congenital TTP [7]. Here, we report a Japanese man with congenital TTP confirmed by genetic analysis, who was followed up for 19 years after initiation of hemodialysis.

Case presentation

A 22-year-old man was admitted to our hospital for renal transplantation. He was the third of five children of non-consanguineous parents. There was no history of severe neonatal jaundice. Purpura of the lower extremities, thrombocytopenia, and proteinuria occurred without any precipitating cause at the age of 6 years, and hemolytic uremic syndrome (HUS) was diagnosed. This episode subsided spontaneously without treatment, but there were repeated recurrences and his renal function deteriorated gradually. In 1990, at the age of 22 years, hemodialysis was started for end-stage renal disease (ESRD) along with the occurrence of cerebral infarction. After 4 months, living-related kidney transplantation was performed with his mother as the donor. Immunosuppressive therapy included prednisolone (70 mg daily), cyclosporine (420 mg daily), antilymphocyte globulin (1 g daily), and azathioprine (100 mg daily). At 7 days after surgery, he developed thrombocytopenia (23.1 to $1.8 \times 10^4/\mu L$) and hemolytic anemia (Hb: 10.3 to 8.2 g/dL), along with an increase of serum creatinine (1.1 to 2.1 mg/dL), lactate dehydrogenase (LDH: 208 to 785 IU), and total bilirubin (0.4 to 2.2 mg/dL). Haptoglobulin was decreased to 3.4 mg/dL. Serum levels of C3 and C4 were also decreased (C3: 63.0 to 51.7 mg/dL, normal range; 83 to 177 mg/dL, C4: 34.4 to 22.9, normal range; 15 to 45 mg/dL). Activation of HUS was suspected to have been caused by cyclosporine, so it was switched to deoxyspergualin (200 mg daily). After methylprednisolone pulse therapy (500 mg/day for 3 days) and infusion of fresh frozen plasma (FFP) (800 mL × 5 days), HUS subsided temporarily. However, there was frequent relapse of HUS, so azathioprine was changed to mizoribine and muromonab-CD3 was administered. Plasma exchange or infusion FFP was effective for terminating each episode of HUS. After 50 days, cerebral hemorrhage occurred, followed by gastrointestinal bleeding at 90 days. Then HUS recurred with thrombocytopenia and hemolytic anemia, which was refractory to plasma exchange or infusion of FFP, and his renal function deteriorated gradually. In May 1991, removal of the kidney graft was performed and hemodialysis was restarted. Examination of the resected kidney showed thrombi, endothelial cell swelling, and numerous red blood cells in the glomeruli and small arteries (Figure 1). After nephrectomy, jejunal bleeding was treated by transcatheter arterial embolization of an arteriovenous malformation in the superior mesenteric artery territory.

Even after hemodialysis was resumed, transient ischemic attacks and cerebral infarction occurred every time his platelet count decreased spontaneously, subsiding in response to infusion of FFP. However, TTP became refractory to FFP in 1998. Because indium platelet scintigraphy showed high uptake in the spleen and his platelets had a short lifespan (1.76 days), splenectomy was performed in order to prevent excessive platelet destruction. Thereafter, thrombotic episodes requiring the infusion of FFP did not occur for 10 years until 2008. During this remission period, the serum level of C3 was always lower than normal and serum C4 was normal, while the C3 level decreased much further with each episode of TTP. When cerebral infarction with thrombocytopenia occurred again at the age of 39 years, plasma ADAMTS13 activity was less than 5% of normal, as measured by the FRETS-VWF73 assay [8], while ADAMTS13 inhibitor was negative (<0.5 Bethesda units/mL) [9]. USS was diagnosed because he had severe deficiency of ADAMTS13 activity without any detectable inhibitor in conjunction with appropriate clinical criteria. Although the thrombotic episodes subsided following infusion of FFP, he died suddenly after hemodialysis in 2010 at the age of 41 years. After the patient's death, we measured plasma ADAMTS13 activity and inhibitor in his parents using a chromogenic ELISA [10]. Both of them had ADAMTS13 activity around 30% of normal and the inhibitor was negative.

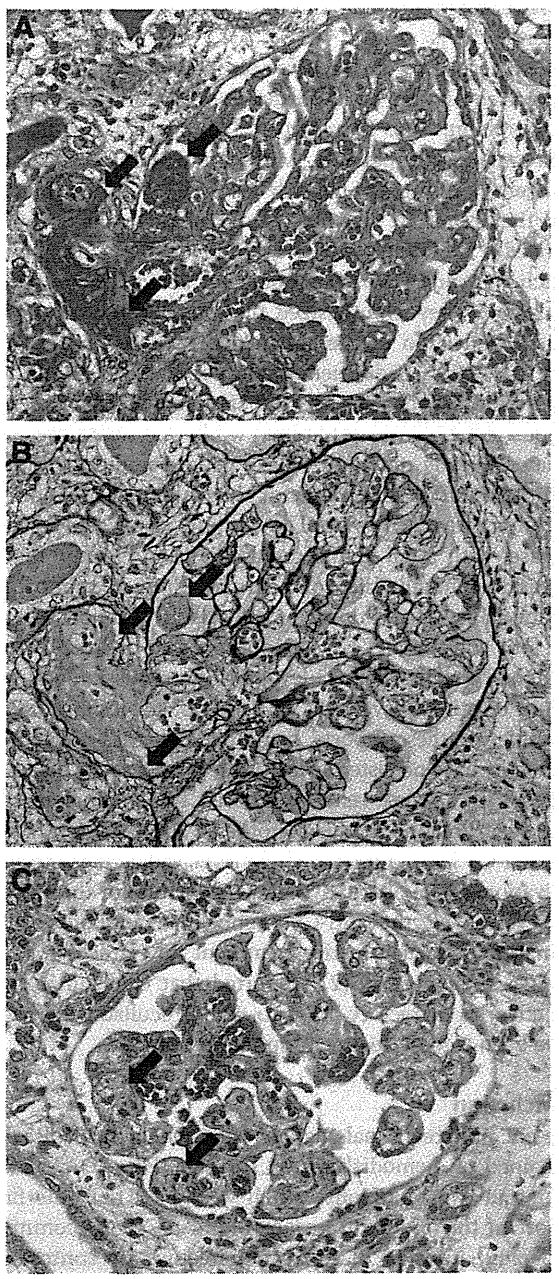

Figure 1 Renal histopathological findings. A, B: Fibrin thrombi in small arteries (arrows) and a glomerulus containing numerous red blood cells (**A**: Heidenhain's azan trichrome stain, **B**: Periodic acid methenamine silver stain × 400). **C:** Endothelial cell swelling (arrows) (Heidenhain's azan trichrome stain × 400).

Genetic analysis

After obtaining consent from his parents, genetic analysis of the patient and parents was performed with the approval of the Ethics Committees of Nara Medical University, the National Cerebral and Cardiovascular Center, and Toranomon Hosipital. Genetic analysis of the patient was carried out at the National Cerebral and Cardiovascular Center using DNA extracted from the resected spleen. For his parents, analysis was performed at the Department of Blood Transfusion Medicine of Nara Medical University.

It was demonstrated that the patient had compound heterozygous mutations of ADAMTS13, comprising a missense mutation in exon 26 (c.3650T>C causing p. I1217T) that was inherited from his father and a missense mutation in exon 21 (c.2723G>A causing p.C908Y) inherited from his mother. A diagnosis of congenital TTP (USS) was confirmed by these findings (Figure 2).

Discussion

It is widely recognized that TTP is associated with renal abnormalities, with renal failure occurring secondary to damage caused by microthrombi that develop because of decreased plasma ADAMTS13 activity. The common renal manifestations of TTP are proteinuria and hematuria. Acute renal failure (ARF) affects 11% of patients with severe congenital TTP and often recurs with exacerbation of this disease [7]. Although ARF requiring dialysis was reported to be less frequent (0–9.7%) in four series of patients with acquired TTP [11-13], the percentage of patients with congenital TTP who need regular dialysis is unclear. Tsai et al. [7] reported that five out of nine patients with USS progressed to ESRD requiring dialysis, and three of them had episodes of ARF. Therefore, repeated episodes of ARF may be associated with progression to ESRD.

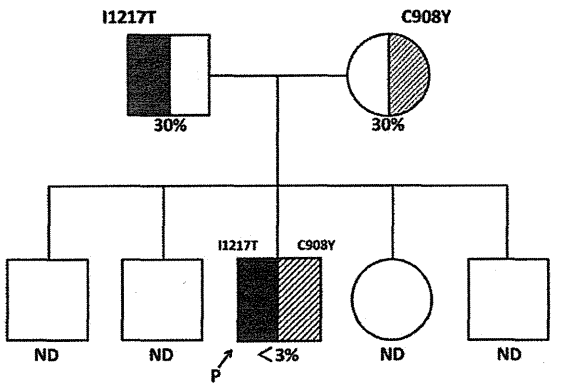

Figure 2 Pedigree of the index patient with genetic haplotypes and plasma activity of ADAMTS13 (a disintegrin and metalloprotease with thrombospondin type I domain 13). Squares represent males and circles represent females. Plasma ADAMTS13 activity (%) is shown under the circles and squares. Mutations of the ADAMTS13 gene are shown as one-letter amino acid abbreviations numbered from the initial Met codon. The arrow indicates the index patient. The mother and father of the index patient are both asymptomatic carriers. Abbreviations P: patient, ND: not determined.

Because infusion of plasma is effective for acute exacerbation of congenital TTP, plasma exchange is the standard treatment. In patients with relapsing and/or refractory TTP, splenectomy can be effective. The mechanism is assumed to be that splenectomy decreases autoantibody production by removing a large reservoir of B lymphocytes [14], which is a reasonable explanation for patients with acquired TTP and elevated levels of ADAMTS13 inhibitor. However, Snider et al. [15] reported a patient with relapsing and refractory congenital TTP who remained in complete clinical remission for 4 years after splenectomy. In our patient, remission of TTP persisted for 10 years after splenectomy, but the effect was limited. The mechanism by which splenectomy improves congenital TTP is unknown, although it is possible that a state like idiopathic thrombocytopenia purpura (ITP) might have coexisted with TTP in our patient because his short platelet lifespan was compatible with ITP. Since TTP remained in remission for 10 years after splenectomy without the need for FFP, this case shows that splenectomy can be a useful option for relapsing/refractory congenital TTP. There has only been one previous case report of renal transplantation for chronic renal failure in a patient with congenital TTP, and the graft showed early failure due to disease recurrence [16]. In our case, the graft also failed due to chronic relapsing TTP only 5 months after transplantation. Therefore, renal transplantation may not a feasible option for ESRD in patients with congenital TTP.

Several mutations of the ADAMTS13 gene have been reported in congenital TTP. It is thought that specific ADAMTS13 mutations are more common among certain ethnicities [17]. Fujimura et al. [17] evaluated 43 USS patients in Japan and found ADAMTS13 mutations that were specific to Japanese individuals with congenital TTP. The present patient had p.C908Y with maternal inheritance, which is one of the common ADAMTS13 mutations found in Japanese patients [17]. However, the patient also had p.I1271T (inherited from his father) and this has not been reported before in Japanese patients, was although it is consistent with the missense mutation reported by Park et al. [18] in a Korean patient who had congenital TTP complicating moyamoya disease. Fujimura et al. [17] reported that two out of 43 patients with congenital TTP progressed to ESRD requiring dialysis. One of them was homozygous for c.414 + 1G > A, while the other was heterozygous for c.1885delT (paternal inheritance) and p.C908Y (maternal inheritance). However, these mutations were also detected in some of their TTP patients without progression to dialysis. In fact, five of the 43 patients had the p.C908Y mutation that was detected in our case, but only one of them progressed to dialysis during follow-up. Therefore, as Tsai et al. [7] concluded, the relation between ADAMTS13 mutation and the renal prognosis remains uncertain [17].

With regard to the occurrence of renal impairment in this patient, it may be important to focus on the complement system. Ruiz-Torres et al. [19] studied thrombotic microangiopathy patients with congenital ADAMTS13 deficiency and patients with ADAMTS 13 inhibitors, and they reported that four of out of six patients (66%) showed a moderate decrease of C3 in the acute phase, which was indicative of complement activation and consumption. They hypothesized that platelet microthrombi caused activation of the alternative pathway in patients with ADAMTS13 deficiency. Moreover, Noris et al. [20] reported 2 sisters who had the same compound heterozygous ADAMTS13 mutations, while one sister also had a heterozygous mutation of the gene encoding complement factor H, a plasma factor that inhibits activation of the alternative pathway. The second sister had severe disease, with renal involvement requiring chronic dialysis, and eventually died of a stroke. She had subnormal serum C3 levels and normal C4 levels. In addition, one of the four congenital TTP patients reported by Ruiz-Torres et al. had a subnormal C3 level even in remission and her serum creatinine level was 5.73 mg/dL, suggesting ESRD. Considering these reports, some patients with congenital TTP may have persistently low C3 levels that may be associated with a worse renal prognosis. The findings in our case seem to support this hypothesis. If a persistently depressed C3 level and normal C4 level, indicating selective activation of the alternative pathway, is one of the causes of severe TTP, the anti-C5 monoclonal antibody eculizumab may be an effective treatment for refractory TTP. In fact, Chapin et al. [21] reported that eculizumab was effective for refractory TTP, so use of eculizumab might have been a good treatment option in our case.

Conclusion

We encountered a male patient with congenital TTP who remained on hemodialysis for 19 years. His ADAMTS13 gene had two mutations, which were p.I1217T (the first report of this mutation in Japan) and p.C908Y (common in Japan). Infusion of FFP was effective for controlling thrombotic episodes, but the improvement was limited and of short duration. The profile of complement components in this patient suggests an association of persistently low serum C3 level with refractory TTP and a worse renal prognosis.

Consent

Written informed consent was obtained from the patient's parents for the genetic analyses, as well as for publication of this case report and any accompanying images. We could not obtain written consent from the patient himself because he was already dead when we wrote this paper.

Competing interests
The authors declare that they have no competing interests.

Authors' contributions
KM contributed to analyzing and interpretation of data and writing the manuscript. YU contributed to analyzing and interpretation of data and writing the manuscript. MM contributed to analyzing and interpretation of data and writing the manuscript. KS contributed to managing the patient and assessing data. RH contributed to managing the patient and assessing data. EH contributed to managing the patient and assessing data. MY contributed to managing the patient and assessing data. NH contributed to managing the patient and assessing data. TS contributed to managing the patient and assessing data. JH contributed to managing the patient and assessing data. NS contributed to managing the patient and assessing data. KO contributed to analyzing and interpretation of pathological findings. KK contributed to analyzing the ADAMTS13 gene of patient. TM contributed to analyzing the ADAMTS13 gene of patient. YF contributed to analyzing and interpretation of data and writing the manuscript. KT contributed to analyzing and interpretation of data and management the patient. All authors read and approved the final manuscript.

Acknowledgements
This work was partly supported by a grant from the Okinaka Memorial Institute for Medical Research and by grants-in-aid from the Ministry of Health, Labor, and Welfare of Japan; the Ministry of Education, Culture, Sports, Science, and Technology of Japan; the Japan Society for the Promotion of Science; and Takeda Medical Foundation of Japan.

Author details
[1]Nephrology Center, Toranomon Hospital, Tokyo, Japan. [2]Department of Pathology, Toranomon Hospital, Tokyo, Japan. [3]Okinaka Memorial Institute for Medical Research, Toranomon Hospital, Tokyo, Japan. [4]Department of Blood Transfusion Medicine, Nara Medical University, Nara, Japan. [5]Department of Molecular Pathogenesis, National Cerebral and Cardiovascular Center, Suita, Osaka, Japan. [6]Nephrology Center, Toranomon Hospital Kajigaya, 1-3-1, Kajigaya, Takatu-ku, Kawasaki-shi, Kanagawa-ken 213-0015, Japan.

Received: 8 March 2013 Accepted: 9 July 2013
Published: 20 July 2013

References

1. Bianchi V, Robles R, Alberio L, Furlan M, Lammle B: **Von willebrand factor-cleaving protease (ADAMTS13) in thrombocytopenic disorders: a severely deficient activity is specific for thrombotic thrombocytopenic purpura.** *Blood* 2002, **100**(2):710–713.
2. Levy GG, Nichols WC, Lian EC, Foroud T, McClintick JN, McGee BM, Yang AY, Siemieniak DR, Stark KR, Gruppo R, *et al*: **Mutations in a member of the ADAMTS gene family cause thrombotic thrombocytopenic purpura.** *Nature* 2001, **413**(6855):488–494.
3. Ruggeri ZM: **Structure and function of von willebrand factor.** *Thromb Haemost* 1999, **82**(2):576–584.
4. Uemura M, Tatsumi K, Matsumoto M, Fujimoto M, Matsuyama T, Ishikawa M, Iwamoto TA, Mori T, Wanaka A, Fukui H, *et al*: **Localization of ADAMTS13 to the stellate cells of human liver.** *Blood* 2005, **106**(3):922–924.
5. Zhou W, Inada M, Lee TP, Benten D, Lyubsky S, Bouhassira EE, Gupta S, Tsai HM: **ADAMTS13 is expressed in hepatic stellate cells.** *Lab Invest* 2005, **85**(6):780–788.
6. Manea M, Kristoffersson A, Schneppenheim R, Saleem MA, Mathieson PW, Morgelin M, Bjork P, Holmberg L, Karpman D: **Podocytes express ADAMTS13 in normal renal cortex and in patients with thrombotic thrombocytopenic purpura.** *Br J Haematol* 2007, **138**(5):651–662.
7. Tsai HM: **The kidney in thrombotic thrombocytopenic purpura.** *Minerva Med* 2007, **98**(6):731–747.
8. Kokame K, Nobe Y, Kokubo Y, Okayama A, Miyata T: **FRETS-VWF73, a first fluorogenic substrate for ADAMTS13 assay.** *Br J Haematol* 2005, **129**(1):93–100.
9. Furlan M, Robles R, Galbusera M, Remuzzi G, Kyrle PA, Brenner B, Krause M, Scharrer I, Aumann V, Mittler U, *et al*: **von willebrand factor-cleaving protease in thrombotic thrombocytopenic purpura and the hemolytic-uremic syndrome.** *N Engl J Med* 1998, **339**(22):1578–1584.
10. Kato S, Matsumoto M, Matsuyama T, Isonishi A, Hiura H, Fujimura Y: **Novel monoclonal antibody-based enzyme immunoassay for determining plasma levels of ADAMTS13 activity.** *Transfusion* 2006, **46**(8):1444–1452.
11. Vesely SK, George JN, Lammle B, Studt JD, Alberio L, El-Harake MA, Raskob GE: **ADAMTS13 Activity in thrombotic thrombocytopenic purpura-hemolytic uremic syndrome: relation to presenting features and clinical outcomes in a prospective cohort of 142 patients.** *Blood* 2003, **102**(1):60–68.
12. Raife T, Atkinson B, Montgomery R, Vesely S, Friedman K: **Severe deficiency of VWF-cleaving protease (ADAMTS13) activity defines a distinct population of thrombotic microangiopathy patients.** *Transfusion* 2004, **44**(2):146–150.
13. Zheng XL, Kaufman RM, Goodnough LT, Sadler JE: **Effect of plasma exchange on plasma ADAMTS13 metalloprotease activity, inhibitor level, and clinical outcome in patients with idiopathic and nonidiopathic thrombotic thrombocytopenic purpura.** *Blood* 2004, **103**(11):4043–4049.
14. Bouw MC, Dors N, van Ommen H, Ramakers-van Woerden NL: **Thrombotic thrombocytopenic purpura in childhood.** *Pediatr Blood Cancer* 2009, **53**(4):537–542.
15. Snider CE, Moore JC, Warkentin TE, Finch CN, Hayward CP, Kelton JG: **Dissociation between the level of von willebrand factor-cleaving protease activity and disease in a patient with congenital thrombotic thrombocytopenic purpura.** *Am J Hematol* 2004, **77**(4):387–390.
16. Veyradier A, Lavergne JM, Ribba AS, Obert B, Loirat C, Meyer D, Girma JP: **Ten candidate ADAMTS13 mutations in six french families with congenital thrombotic thrombocytopenic purpura (upshaw-schulman syndrome).** *J Thromb Haemost* 2004, **2**(3):424–429.
17. Fujimura Y, Matsumoto M, Isonishi A, Yagi H, Kokame K, Soejima K, Murata M, Miyata T: **Natural history of upshaw-schulman syndrome based on ADAMTS13 gene analysis in Japan.** *J Thromb Haemost* 2011, **9**(Suppl 1):283–301.
18. Park HW, Oh D, Kim N, Cho HY, Moon KC, Chae JH, Ahn HS, Choi Y, Cheong HI: **Congenital thrombotic thrombocytopenic purpura associated with unilateral moyamoya disease.** *Pediatr Nephrol* 2008, **23**(9):1555–1558.
19. Ruiz-Torres MP, Casiraghi F, Galbusera M, Macconi D, Gastoldi S, Todeschini M, Porrati F, Belotti D, Pogliani EM, Noris M, *et al*: **Complement activation: the missing link between ADAMTS-13 deficiency and microvascular thrombosis of thrombotic microangiopathies.** *Thromb Haemost* 2005, **93**(3):443–452.
20. Noris M, Bucchioni S, Galbusera M, Donadelli R, Bresin E, Castelletti F, Caprioli J, Brioschi S, Scheiflinger F, Remuzzi G: **Complement factor H mutation in familial thrombotic thrombocytopenic purpura with ADAMTS13 deficiency and renal involvement.** *J Am Soc Nephrol* 2005, **16**(5):1177–1183.
21. Chapin J, Weksler B, Magro C, Laurence J: **Eculizumab in the treatment of refractory idiopathic thrombotic thrombocytopenic purpura.** *Br J Haematol* 2012, **157**(6):772–774.

doi:10.1186/1471-2369-14-156
Cite this article as: Mise *et al.*: Long term follow up of congenital thrombotic thrombocytopenic purpura (Upshaw-Schulman syndrome) on hemodialysis for 19 years: a case report. *BMC Nephrology* 2013 14:156.

Thrombosis Research 132 (2013) 314–315

Contents lists available at ScienceDirect

Thrombosis Research

journal homepage: www.elsevier.com/locate/thromres

Letter to the Editors-in-Chief

Protein S K196E mutation, a genetic risk factor for venous thromboembolism, is limited to Japanese

Dear Editors,

Ethnic differences in thrombotic genetic risk have received much attention in recent years because the established thrombotic genetic variants, factor V Leiden and prothrombin G20210A mutation, are limited in Caucasian populations but not in East Asian populations [1]. We and others have identified the protein S K196E mutation (rs121918474) as a genetic risk factor for venous thromboembolism (VTE) in a Japanese population with odds ratios between 3.74 and 8.56 [2–5]. The allele frequency of this mutation is 0.0089 [5,6]. When overlapping with congenital protein C deficiency, this mutation facilitates the development of VTE [4,7]. The individuals heterozygous for the mutant E-allele had 16% lower protein S anticoagulant activity than wild-type subjects [8]. An *in vitro* study showed that the recombinant protein S with the K196E mutation lost activated protein C-dependent anticoagulant activity [9]. Since East Asians including Japanese, Chinese, and Koreans are geographically and genetically close, the protein S K196E mutation, which has so far been found only in Japanese, may be found in other East Asians. In this study, we have genotyped the protein S K196E mutation in Chinese and Korean populations to clarify the geographic distribution of this thrombotic mutation. The mutation was not found in Chinese or Koreans.

The first panel for the genotyping was a general Chinese population consisting of 509 individuals: 50 in Dehui, 49 in Huludao, 50 in Beijing, 49 in Jinan, 50 in Xi'an, 47 in Baoji, 50 in Shanghai, 50 in Changsha, 15 in Heping, 50 in Nanning, and 49 in Tainan. The second panel was a general Korean population consisting of 492 individuals including 105 in Seoul, 29 in Chonan, 46 in Haman, 247 in Pusan, and 65 in Jeju-do [10,11]. The third panel consisted of 122 Chinese patients with VTE and 112 Chinese control individuals [12]. Furthermore, from the 1000 Genomes Project (http://www.1000genomes.org/) we retrieved the genetic information of protein S K196E mutation in 197 Chinese consisting of 97 Chinese in Beijing and 100 Chinese in southern China, as well as in 89 Japanese [13].

The genotype of protein S K196E mutation in the first two panels was determined by the TaqMan genotype discrimination method [8] using the primers 5'- ACCACTGTTCCTGTAAAAATGGTTT/5'- TTTAATT CTACCATCCTGCTCTTACCT and the probes 5'-FAM - CAATCTTTCTtAT TTGAAAGC-MGB (the wild-type allele)/5'-VIC- AATCTTTCTcATTTGA AAGC (the mutant allele). In the third panel, we genotyped the mutation by the Homogeneous Mass Extend and iPLEX assays (Sequenom, Hamburg, Germany) and validated it with the SNaPshot assay (Applied Biosystems, USA). Primer sequences of the SEQUENOM assay are available on request. The PCR primers for the SNaPshot were AGACATAA ATGAACGCAAAGATC and TCTAACTGGGATTATTCTCACAC, and the sequence for the extension probe was TTTTTTTTTTTTTTCTTACCTTTACA GTCTTTCT. The SNaPshot products were resolved and analyzed using an ABI 3730 Automated Sequence Analyzer (Applied Biosystems). The study protocol was approved by the Institutional Review Boards and Ethics Committees of Kyoto University School of Medicine and by the General Hospital of the People's Liberation Army.

We genotyped the protein S K196E mutation in 509 Chinese and 492 Koreans and found that none carried the mutation. We did not identify the mutation in 122 Chinese patients with VTE or in 112 Chinese control individuals. Thus, the genetic analysis of three independent panels indicated that the protein S K196E mutation is present solely in Japanese and not in Chinese. The number of Korean individuals we genotyped was insufficient to yield conclusive evidence, and the 1000 Genomes Project does not include Koreans, but it is likely that Koreans also do not carry the mutation. The 1000 Genomes Project showed that none of the 197 Chinese carried the protein S K196E mutation, but one heterozygous carrier was present in 89 Japanese. We calculated a statistical power to detect a difference of minor allele frequency between Japanese and Chinese/Korean with the 0.05 level of significance. A one-sided statistical power more than 0.80 was considered statistically significant. Albeit a large enough statistical power for Chinese (0.82), a low statistical power, 0.67, for Korean may permit us to apply above argument to only Chinese.

The finding that the protein S K196E mutation is present only in Japanese was unexpected, because in thrombosis-related factors, two genetic mutations found in Japanese but not in Caucasians, plasminogen A620T and ADAMTS13 P475S, are both present in Chinese and Koreans [14,15]. The present results suggest that, even though Japanese, Chinese, and Koreans are geographically close to one another, the genetic background for thrombosis differs among them. The results also suggest that the protein S K196E mutation is a recent occurrence and fixed within the Japanese population.

Conflict of Interest Statement

The authors state that they have no conflict of interest.

Acknowledgments

We thank Dr. Hiroko Shirotani-Ikejima for her excellent technical assistance. This work was supported in part by grants-in-aid from the Ministry of Health, Labour, and Welfare of Japan; the Ministry of Education, Culture, Sports, Science, and Technology of Japan; the Japan Society for the Promotion of Science; and by the National Natural Science Foundation of China (No. 30971259). The research activity of X. P. Fan, of the Beijing Chaoyang Hospital affiliated with the Capital Medical University of China, was supported by a Scholarship from the Takeda Foundation.

References

[1] Zakai NA, McClure LA. Racial differences in venous thromboembolism. J Thromb Haemost 2011;9:1877–82.
[2] Kinoshita S, Iida H, Inoue S, Watanabe K, Kurihara M, Wada Y. Protein S and protein C gene mutations in Japanese deep vein thrombosis patients. Clin Biochem 2005;38:908–15.

0049-3848/$ – see front matter
http://dx.doi.org/10.1016/j.thromres.2013.05.008

[3] Kimura R, Honda S, Kawasaki T, Tsuji H, Madoiwa S, Sakata Y, et al. Protein S-K196E mutation as a genetic risk factor for deep vein thrombosis in Japanese patients. Blood 2006;107:1737–8.
[4] Ikejiri M, Wada H, Sakamoto Y, Ito N, Nishioka J, Nakatani K, et al. The association of protein S Tokushima-K196E with a risk of deep vein thrombosis. Int J Hematol 2010;92:302–5.
[5] Miyata T, Kimura R, Kokubo Y, Sakata T. Genetic risk factors for deep vein thrombosis among Japanese: importance of protein S K196E mutation. Int J Hematol 2006;83: 217–23.
[6] Miyata T, Hamasaki N, Wada H, Kojima T. More on: racial differences in venous thromboembolism. J Thromb Haemost 2012;10:319–20.
[7] Miyata T, Sato Y, Ishikawa J, Okada H, Takeshita S, Sakata T, et al. Prevalence of genetic mutations in protein S, protein C and antithrombin genes in Japanese patients with deep vein thrombosis. Thromb Res 2009;124:14–8.
[8] Kimura R, Sakata T, Kokubo Y, Okamoto A, Okayama A, Tomoike H, et al. Plasma protein S activity correlates with protein S genotype but is not sensitive to identify K196E mutant carriers. J Thromb Haemost 2006;4:2010–3.
[9] Hayashi T, Nishioka J, Suzuki K. Molecular mechanism of the dysfunction of protein S(Tokushima) (Lys155– > Glu) for the regulation of the blood coagulation system. Biochim Biophys Acta 1995;1272:159–67.
[10] Liu W, Morito D, Takashima S, Mineharu Y, Kobayashi H, Hitomi T, et al. Identification of RNF213 as a susceptibility gene for moyamoya disease and its possible role in vascular development. PLoS One 2011;6:e22542.
[11] Liu W, Hitomi T, Kobayashi H, Harada KH, Koizumi A. Distribution of moyamoya disease susceptibility polymorphism p.R4810K in RNF213 in East and Southeast Asian Populations. Neurol Med Chir (Tokyo) 2012;52:299–303.
[12] Xu Q, Xu B, Zhang Y, Yang J, Gao L, Wang H, et al. Estimation of the warfarin dose with a pharmacogenetic refinement algorithm in Chinese patients mainly under low-intensity warfarin anticoagulation. Thromb Haemost 2012;108:1132–40.
[13] Abecasis GR, Auton A, Brooks LD, DePristo MA, Durbin RM, Handsaker RE, et al. An integrated map of genetic variation from 1,092 human genomes. Nature 2012;491:56–65.
[14] Ooe A, Kida M, Yamazaki T, Park SC, Hamaguchi H, Girolami A, et al. Common mutation of plasminogen detected in three Asian populations by an amplification refractory mutation system and rapid automated capillary electrophoresis. Thromb Haemost 1999;82:1342–6.
[15] Ruan C, Dai L, Su J, Wang Z. The frequency of P475S polymorphism in von Willebrand factor-cleaving protease in the Chinese population and its relevance to arterial thrombotic disorders. Thromb Haemost 2004;91:1257–8.

Wanyang Liu
Department of Health and Environmental Sciences, Kyoto University Graduate School of Medicine, Kyoto, Japan
Department of Occupational and Environmental Health, School of Public Health, China Medical University, Shenyang, China

Tong Yin
Yang Li
Bin Xu
Jie Yang
Hongjuan Wang
Institute of Geriatric Cardiology, General Hospital of Chinese People's Liberation Army, Beijing, China

Hiroko Okuda
Kouji H. Harada
Akio Koizumi
Department of Health and Environmental Sciences, Kyoto University Graduate School of Medicine, Kyoto, Japan

Xinping Fan
Department of Molecular Pathogenesis, National Cerebral and Cardiovascular Center, Suita, Osaka, Japan
Department of Clinical Laboratory, Beijing Chaoyang Hospital, Capital Medical University, Beijing, China

Toshiyuki Miyata
Department of Molecular Pathogenesis, National Cerebral and Cardiovascular Center, Suita, Osaka, Japan
Corresponding author. Tel.: +81 6 6833 5012; fax: +81 6 6835 1176.
E-mail address: miyata@ri.ncvc.go.jp.

27 March 2013

OPEN ACCESS Freely available online

PLOS | ONE

The Integrin-Linked Kinase-PINCH-Parvin Complex Supports Integrin αIIbβ3 Activation

Shigenori Honda[1*], Hiroko Shirotani-Ikejima[1], Seiji Tadokoro[2], Yoshiaki Tomiyama[2,3], Toshiyuki Miyata[1]

1 Department of Molecular Pathogenesis, National Cerebral and Cardiovascular Center, Suita, Japan, **2** Department of Hematology and Oncology, Osaka University Graduate School of Medicine, Suita, Osaka, Japan, **3** Department of Blood Transfusion, Osaka University Hospital, Suita, Osaka, Japan

Abstract

Integrin-linked kinase (ILK) is an important signaling regulator that assembles into the heteroternary complex with adaptor proteins PINCH and parvin (termed the IPP complex). We recently reported that ILK is important for integrin activation in a Chinese hamster ovary (CHO) cell system. We previously established parental CHO cells expressing a constitutively active chimeric integrin (αIIbα6Bβ3) and mutant CHO cells expressing inactive αIIbα6Bβ3 due to ILK deficiency. In this study, we further investigated the underlying mechanisms for ILK-dependent integrin activation. ILK-deficient mutant cells had trace levels of PINCH and α-parvin, and transfection of ILK cDNA into the mutant cells increased not only ILK but also PINCH and α-parvin, resulting in the restoration of αIIbα6Bβ3 activation. In the parental cells expressing active αIIbα6Bβ3, ILK, PINCH, and α-parvin were co-immunoprecipitated, indicating the formation of the IPP complex. Moreover, short interfering RNA (siRNA) experiments targeting PINCH-1 or both α- and β-parvin mRNA in the parent cells impaired the αIIbα6Bβ3 activation as well as the expression of the other components of the IPP complex. In addition, ILK mutants possessing defects in either PINCH or parvin binding failed to restore αIIbα6Bβ3 activation in the mutant cells. Kindlin-2 siRNA in the parental cells impaired αIIbα6Bβ3 activation without disturbing the expression of ILK. For CHO cells stably expressing wild-type αIIbβ3 that is an inactive form, overexpression of a talin head domain (THD) induced αIIbβ3 activation and the THD-induced αIIbβ3 activation was impaired by ILK siRNA through a significant reduction in the expression of the IPP complex. In contrast, overexpression of all IPP components in the αIIbβ3-expressing CHO cells further augmented THD-induced αIIbβ3 activation, whereas they did not induce αIIbβ3 activation without THD. These data suggest that the IPP complex rather than ILK plays an important role and supports integrin activation probably through stabilization of the active conformation.

Citation: Honda S, Shirotani-Ikejima H, Tadokoro S, Tomiyama Y, Miyata T (2013) The Integrin-Linked Kinase-PINCH-Parvin Complex Supports Integrin αIIbβ3 Activation. PLoS ONE 8(12): e85498. doi:10.1371/journal.pone.0085498

Editor: Maddy Parsons, King's College London, United Kingdom

Received August 3, 2013; **Accepted** December 5, 2013; **Published** December 23, 2013

Funding: This work was supported in part by grants from the Ministry of Health, Labor, and Welfare of Japan; and from the Ministry of Education, Culture, Sports, Science, and Technology of Japan. The funders had no role in study design, data collection and analysis, decision to publish, or preparation of the manuscript.

Competing interests: The authors have declared that no competing interests exist.

* E-mail: shige@ncvc.go.jp

Introduction

Cell adhesions are critical for hemostasis processes composed of interactions between vessel walls, platelets and coagulation-related proteins. During these processes, cells react with several elements such as extracellular matrix (ECM) proteins and cell surface receptors. As one of the main elements, an integrin family is known to play a key role in cell-ECM interactions. Integrins, transmembrane glycoprotein adhesion receptors, are composed of α and β subunits and are linked non-covalently. Both subunits include long extracellular domains, transmembrane domains, and short cytoplasmic domains. There are at least two conformational states of integrin presenting low affinity (inactive) or high affinity (active) against its ligands and this heterodimeric receptor acts as a bidirectional signaling transducer. The binding of the cytoplasmic proteins such as talin and kindlins to the integrin β cytoplasmic domain upregulates the ligand-binding affinity of integrin (inside-out signaling). In contrast, ligand binding to integrins and the subsequent clustering of ligand-bound integrins result in intracellular molecular rearrangements such as focal adhesion formation and cell spreading (outside-in signaling) [1].

αIIbβ3, a major integrin expressed on platelets, is critical for platelet aggregation mediated by bindings of fibrinogen and von Willebrand factor. Since inside-out signaling pathways of αIIbβ3 induce striking conformational changes between inactive and active states, the activation processes of αIIbβ3 have been extensively investigated [2]. Talin, a cytoskeletal protein consisting of an N-terminal head and a C-terminal rod,

has been well characterized as an integrin activator [3,4]. The talin head domain (THD) contains four subdomains: F0, F1, F2, and F3. The F3 domain itself can bind to the β3 cytoplasmic domain and exert αIIbβ3 activation [5]. Other subdomains also have important roles in the activation [6-8]. The kindlin family members (kindlin-1, -2, and -3), which are focal adhesion proteins, have recently been proven to be critical for integrin activation [9,10]. Kindlin-1 and -2 are widely expressed and kindlin-3 expression is restricted mainly to hematopoietic cells [11]. Several studies suggest that the binding of talin and kindlins to the integrin β3 cytoplasmic domain is pivotal for the final step in the inside-out activation of αIIbβ3. Moreover, since kindlins synergistically augment talin-dependent αIIbβ3 activation, they act as a co-activator of talin [12,13]. However, regulatory molecules other than talin and kindlins necessary to αIIbβ3 activation remain to be fully clarified.

Since platelets are inadequate for gene manipulation, the CHO cell system has been used to study essential regulators of integrin αIIbβ3 function. For example, αIIbβ3-expressing CHO cells contributed to the elucidation of the functional importance of kindlin-1 and -2 as co-activators and of THD as a direct activator of integrin [10,12]. It was also shown that the Rap1-GTP-interacting adaptor molecule promotes talin-dependent integrin activation in the CHO cell system [14]. A chimeric integrin, αIIbα6Aβ3β1 or αIIbα5β3, expressed on CHO cells having the extracellular and transmembrane domains of αIIbβ3 connected to the cytoplasmic domains of α6Aβ1or α5β3 has been constitutively active on CHO cells but susceptible to integrin regulatory proteins [15]. Several integrin regulatory proteins including H-ras, PEA-15, CD98, and talin were characterized in this cell system [15-18]. Thus, the CHO cell system has been utilized to analyze the mechanisms by which integrin function is regulated.

Integrin-linked kinase (ILK) was originally identified as a serine/threonine kinase associated with integrin β1 and β3 cytoplasmic domains. It consists of three domains: an N-terminal ankyrin repeat domain, a putative pleckstrin homology domain, and a C-terminal kinase domain [19]. Many studies have shown that ILK is widely expressed and involved in interactions between integrins, cytoskeletal proteins, and signaling molecules. A deficiency or aberrant function of ILK resulted in the impairment of adhesion, spreading, migration, proliferation, and survival of the cells [20]. ILK seems to have two functions: that of a scaffold protein and that of a protein kinase, whereas the kinase activity is controversial [21,22]. At focal adhesion sites, ILK forms a heterotrimeric complex composed of the adaptor proteins PINCH and parvin [23-28]. PINCH consists of two members, PINCH-1 and -2, each of which consists of five LIM domains. PINCH-1 and -2 are ubiquitously expressed in mammalian tissues and show overlapping expression in many tissues. Parvin comprises three members, α-, β-, and γ-parvin, and contains N-terminal nuclear localization sequences and two calponin homology domains. In mammalian tissues, α- and β-parvin are ubiquitously expressed but γ-parvin is expressed mainly in hematopoietic tissues. These adaptor proteins are known to directly bind to several cytoplasmic proteins including Nck2 for PINCH and filamentous actin for parvin [25,29]. The ankyrin repeat domain of ILK binds to PINCH and the kinase domain binds to parvin. ILK interacts directly or indirectly with several other cytoskeletal and signaling proteins and exerts diverse roles in different tissues [30].

In our previous study, we identified ILK as a molecule important for integrin activation, using an expression cloning system as follows. First, we established CHO cells expressing constitutively active integrin αIIbα6Bβ3 whose αIIb cytoplasmic domain we replaced by that of integrin α6B (parental cells). Next we obtained mutant cells with inactive integrin using genome-wide mutagenesis, and finally isolated an ILK cDNA was isolated as a factor that complements the function of inactive αIIbα6Bβ3 in mutant cells by expression cloning [31]. Although the role of ILK at focal adhesion sites has been well studied, there are only a few reports on the involvement of ILK in integrin activation [32,33]. In the present study, we further investigated the mechanisms by which ILK regulates integrin activation in the CHO cell system.

Materials and Methods

Plasmids

Human wild-type (WT) αIIb and β3 subcloned into expression plasmid pcDNA3 (Invitrogen, San Diego, CA) were provided by Drs P. Newman and G. White (Blood Research Institute, Blood Center of Wisconsin, Milwaukee, WI). pRKHA, including full-length mouse talin-1 was a gift from Dr K. Yamada (NIH, Bethesda, MD). The N-terminal head region (residues 1-433) of talin-1 was constructed by polymerase chain reaction (PCR) and subcloned into green fluorescence protein (GFP) containing vector pEGFP-N1 to make a fusion protein of THD with GFP (THD-GFP) (Clontech, Mountain View, CA). Mouse α-parvin cDNA and mouse PINCH-1 cDNA (Thermo Scientific Open Biosystems, Lafayette, CO) were amplified by PCR and then were subcloned into expression plasmids, pcDNA3.1 (Invitrogen) for α-parvin and pBApo-CMV Pur DNA (Takara Bio, Shiga, Japan) for PINCH-1. pcDNA3-αIIbα6B was created using PCR-based mutagenesis as previously described [31]. Nucleotide and amino acid numbers begin with the start codon (ATG) and the first Met residue, respectively. The full length of rat ILK cDNA was amplified by PCR then subcloned into pcDNA3 and GFP-encoding plasmid pAcGFP1-Hyg-C1 to make a fusion protein of ILK with GFP (GFPILK-WT) (Clontech). Three point mutations (H99D/F109A/W110A) in the ankyrin repeat domain of ILK were introduced into pAcGFP1-Hyg-C1 to make a fusion protein of the ILK mutant with GFP (GFPILK-H99D/F109A/W110A). Two point mutations (M402A/K403A) in the ILK kinase domain were introduced in pAcGFP1-Hyg-C1 to make a fusion protein of the ILK mutant with GFP (GFPILK-M402/K403A). The ILK mutant (H99D/F109A/W110A) was designed to disrupt the PINCH binding based on the crystal structure of a complex of the ankyrin repeat domain of ILK with the LIM1 domain of PINCH, PDB 3F6Q [34]. The ILK mutant (M402A/K403A) was designed to disrupt the parvin binding as previously reported [35]. Expression plasmid pCMV-SPORT6, containing full-length mouse kindlin-2 (Thermo Scientific Open Biosystems) was obtained. All PCR-generated DNA inserts were verified by

sequencing using a BigDye Terminator Cycle Sequencing Kit (Applied Biosystems, Foster City, CA).

Cell Cultures

CHO-K1 cells from ATCC were cultured in DMEM supplemented with 10% fetal bovine serum and 1% non-essential amino acids (Sigma-Aldrich, St. Louis, MO). CHO cells stably expressing constitutively active αIIbα6Bβ3 (parental cells) were previously established [31]. CHO-K1 cells were cotransfected with pcDNA3-αIIbα6B and pcDNA3-β3 using Lipofectamine 2000 (Invitrogen) and selected with 1 mg/ml G418 (Nacalai Tesque, Kyoto, Japan). G418-resistant cells expressing αIIbα6Bβ3 were cloned to isolate parental cells by a limiting dilution method. ILK-deficient mutant cells, which result in its inactive form from active αIIbα6Bβ3 (mutant cells), were previously established by the introduction of random mutations into the parental cells using a chemical mutagen, ethyl methane sulfonate (EMS) [31]. For αIIbβ3-expressing CHO cells, pBApo-CMV Pur DNA-αIIb and pcDNA3-β3 were cotransfected into CHO-K1 cells by Lipofectamine 2000. After selection with 12 μg/ml puromycin (Clontech) and 1 mg/ml G418, clones expressing αIIbβ3 were established by the limiting dilution method.

Flow cytometry

Flow cytometry analyses were performed as previously described [31]. Cells suspended in Tyrode's buffer containing 1.5 mM $CaCl_2$, 1 mM $MgCl_2$, and 1% bovine serum albumin were incubated with the primary antibody of 5 μg/ml of a mouse monoclonal antibody (mAb) specific for αIIbβ3, HIP8 (BD Biosciences) for 30 minutes at 4°C. After washing, the cells were incubated with the secondary Ab of ~1 μg/ml phycoerythrin (PE)-conjugated rat anti-mouse IgG (BD Biosciences) for 30 minutes at 4°C, washed once, stained with 1 μg/ml 7-aminoactinomycin D (7AAD) (Sigma-Aldrich) to discriminate dead cells, and then analyzed on a flow cytometer (FACSCalibur; BD Biosciences). As a negative control, cells were incubated with the secondary Ab alone. For the binding of a ligand-mimetic, activation-specific anti-αIIbβ3 mAb, PAC-1 (BD Biosciences), cells were incubated with 10 μg/ml PAC-1 for 30 minutes at room temperature in the absence or presence of 10 μM of a peptidomimetic antagonist of αIIbβ3, Ro44-9883 (a gift from Astellas Pharma, Tokyo, Japan), washed once, and then incubated with 10 μg/ml PE-conjugated anti-mouse IgM (eBioscience, San Diego, CA) for 30 minutes at 4°C. After washing, cells were stained with 7AAD and then analyzed. As a positive control for PAC-1 binding, cells were incubated with 15 mM dithiothreitol (DTT) for 10 minutes at 37°C to activate integrin αIIbα6Bβ3 and incubated with PAC-1 as mentioned above. Integrin activation was quantified as an activation index calculated using the following formula: 100 x ($F - Fo$) / (Fmax − Fo), where F is the median fluorescence intensity (MFI) of PAC-1 binding, Fo is the PAC-1 binding in the presence of Ro44-9883, and Fmax is the maximal PAC-1 binding in the cells treated with DTT. For fibrinogen binding, cells were incubated with 150 μg/ml Alexa-Fluor 647-conjugated fibrinogen (Molecular Probes, Eugene, OR) under similar conditions to the above assay. In some experiments using αIIbβ3-expressing CHO cells, the activation indexes were normalized by αIIbβ3 expression, as shown by the following formula: 100 x ($F - Fo$) / (F_1 - F_2), where F and Fo are the same as mentioned above, F_1 is the HIP8 binding, and F_2 is the binding of the secondary Ab alone.

Immunoblotting

Immunoblotting was performed using procedures previously described [31]. In brief, cell lysates were subjected to sodium dodecyl sulfate-polyacrylamide gel electrophoresis (SDS-PAGE) and transferred to a polyvinylidene difluoride (PVDF) membrane. The membranes were incubated with either one of the following primary Abs: 0.125 μg/ml mouse mAb specific for ILK, 3/ILK (BD Biosciences), 0.25 μg/ml mouse mAb specific for PINCH, 49/PINCH (BD Biosciences), rabbit polyclonal Ab specific for α-parvin (IgG fraction; 1:3,000) (Sigma-Aldrich), 1 μg/ml mouse mAb specific for β-parvin, 11A5 (Millipore, Temecula, CA), mouse mAb specific for talin, 8D4 (ascites fluid; 1:2,000) (Sigma-Aldrich), rabbit polyclonal Ab specific for kindlin-2 (IgG fraction; 1:1,000) (ProteinTech Group, Chicago, IL), 0.5 μg/ml rabbit polyclonal Ab specific for glyceraldehyde-3-phosphate dehydrogenase (GAPDH), FL-335 (Santa Cruz Biotechnology), horseradish peroxidase (HRP)-conjugated rabbit polyclonal Ab specific for β-actin (IgG fraction; 1:2000) (MBL, Woburn, MA), or 1 μg/ml mouse mAb specific for GFP, B-2 (Santa Cruz Biotechnology) for 90 minutes at room temperature. After washing, bound Abs except for the HRP-conjugated Abs were incubated with peroxidase-conjugated secondary Abs (Kirkegaard & Perry Labs, Gaithersburg, MD) Detection was performed using a chemiluminescence kit (Immobilon Western; Millipore, Bedford, MA). Chemiluminescence was visualized by an image analyzer, LAS-3000PLUS (Fuji Photo Film, Kanagawa, Japan).

Immunoprecipitation

Parental cells were solubilized at concentrations of 2 x 10^7 cells/ml in a lysis buffer (150 mM NaCl, 50 mM Tris-HCl, pH 7.5, and 1% Triton X-100) containing proteinase inhibitors. After centrifugation at 15,000 x g for 12 min, the supernatant (200 μl) was subjected to immunoprecipitation using protein A/G agarose (Santa Cruz Biotechnology) and the following Abs: 1 μg mouse mAb specific for ILK, 3/ILK, 1 μg mouse mAb specific for PINCH, 49/PINCH, 1 μg mouse IgG_1 isotype control, MOPC 21 (Sigma-Aldrich), 1 μg mouse IgG_{2a} isotype control, UPC-10 (Sigma-Aldrich), 1 μg rabbit polyclonal Ab specific for α-parvin, and 1 μg pooled rabbit IgG (Invitrogen). The immunoprecipitants were analyzed by immunoblotting as described above. As a positive control, cell lysates (15 μl) were loaded onto a lane.

Short interfering RNA (siRNA) and transfection

Total RNA from parental cells was extracted with Trizol reagent (Invitrogen). PINCH-1, α- and β-parvin, and kindlin-2 mRNA were amplified by a one-step RT-PCR kit (Qiagen, Valencia, CA) using primers specific to both mouse and rat homologues according to the manufacturer's instructions. RT-PCR products were directly sequenced using specific primers.

siRNAs against RNA targets were designed and synthesized by Invitrogen (Stealth RNAi). The siRNA target sequences of hamster mRNA are as follows: PINCH-1 (p) 157 sense 5'-CGGGUUAUUAAAGCCAUGAACAACA-3'; PINCH-1 (p) 755 sense 5'-CCTGCAATACCAAATTAACACTCAA-3'; α-pavin (pa) 503 sense 5'-CCAGGAGCATCAAGTGGAATGTAGA-3'; α-pavin (pa) 761 sense 5'-CAGACAAGCTCAACGTGGTAAAGAA-3'; β-pavin (pb) 900 sense 5'-UCCACAACUUCUACCUGACACCUGA-3'; β-pavin (pb) 1011 sense 5'-AAGAUGUGGUAAACUUGGACCUCAA-3'; kindlin-2 (k) 770 sense 5'-GAUCGCUAAUGGAACAAGAUGUGUGAA-3'; kindlin-2 (k) 770 scrambled control sense 5'-GAUAUCGUAAAGAACUAGUGCGGAA-3'; kindlin-2 (k) 1733 sense 5'-AAGGCGGCAAGAGAGAAGAACUUAU-3'; kindlin-2 (k) 1733 scrambled control sense 5'-AAGCGGGAAAGAAAGAAGUCGCUAU-3'. The sequences of ILK siRNA (Ilk1255) and its scrambled control were previously described [31]. Stealth RNAi-negative control duplexes (Invitrogen) were used as controls in knockdown experiments targeting PINCH-1 and parvins. Cells cultured in six-well plates were transfected with 12.5-50 nM siRNA using Lipofectamine RNAiMAX (Invitrogen) or cotransfected with 30 nM siRNA and the indicated amounts of plasmid (0.5 μg pEGFP-N1 encoding THD-fused GFP or 0.015 μg pEGFP-N1 plus 0.485 μg pcDNA3 as a negative control) using Lipofectamine 2000. Transfected cells were usually analyzed at 72 hours after transfection. For transfections with plasmid DNA alone, Lipofectamine 2000 was employed.

Statistical analysis

The statistical significance of observed data was determined using one-way analysis of variance followed by Bonferroni's post hoc test using PRISM 5 software (GraphPad Software; La Jolla, CA, USA). P values of 0.05 or less were considered statistically significant.

Results

Evaluation of PINCH, α-parvin, talin, and kindlin-2 in ILK-deficient αIIbα6Bβ3- inactive mutant CHO cells and αIIbα6Bβ3-active parental CHO cells

We previously obtained ILK-deficient mutant cells by treating parental cells expressing constitutively active αIIbα6Bβ3 with the chemical mutagen EMS [31]. In the mutant cells, ILK mRNAs contained two nonsense mutations, R317X and W383X, in a compound heterozygous state, resulting in a complete lack of ILK expression. It has been shown that ILK forms a ternary complex with PINCH and parvins to make an IPP complex [25]. To assess the role of ILK-binding proteins in ILK-deficient mutant cells with the inactive state of αIIbα6Bβ3, we examined the protein expression of ILK-binding adaptor proteins, PINCH and α-parvin. In addition to a lack of ILK expression, mutant cells showed severe reductions in the protein expression of PINCH and α-parvin as compared to parental cells. In contrast, talin and kindlin-2, which play critical roles in integrin activation, were present at normal levels of protein expression (Figure 1A). Transfection of a plasmid encoding ILK cDNA into mutant cells showed the increased expression of ILK and concomitant increases in PINCH and α-parvin expression levels but did not affect talin and kindlin-2 expression levels. Moreover, flow cytometry using an activation-specific anti-αIIbβ3 mAb, PAC-1, showed that ILK-plasmid transfection increased PAC-1 binding compared to empty-plasmid transfection (Figure 1B). These data suggest that ILK, PINCH, and α-parvin are necessary to restore the active state of αIIbα6Bβ3 in mutant cells.

Detection and assessment of ILK, PINCH, and parvin (IPP) complex in αIIbα6Bβ3-active parental cells

Since ILK, PINCH, and parvins form the IPP complex, we assessed IPP complex formation in αIIbα6Bβ3-active parental cells, which show constitutively active αIIbα6Bβ3. Immunoprecipitation experiments revealed that ILK is coprecipitated with PINCH and α-parvin, indicating the presence of the IPP complex in those cells (Figure 2). To evaluate the importance of these proteins comprising the complex on the active state of αIIbα6Bβ3, we performed RNA interference (RNAi) experiments targeting PINCH or parvins, and we analyzed the active state of αIIbα6Bβ3 by flow cytometry using PAC-1. For PINCH siRNA, we targeted PINCH-1, one of the two PINCH isoforms, because we failed to find sequences of PINCH-2 mRNA in CHO cells. Each of the two PINCH-1 siRNAs (p157 and p755) decreased PINCH expression and concomitantly decreased ILK and α-parvin expression compared to nontargeting negative control siRNA in parental cells (Figure 3A), leading to a decreased integrin activation index, which was determined by flow cytometry analysis of PAC-1 binding (Figure 3B). For parvin siRNA, α- and β-parvins were knocked down since both parvins are thought to bind to ILK. A mixture of two α-parvin siRNAs (pa503 and pa761) or two β-parvin siRNAs (pb900 and pb1011) reduced α-parvin or β-parvin expression, respectively; however, ILK and PINCH expression levels were less significantly affected (Figure 3C). When a mixture of α-parvin and β-parvin siRNAs was transfected into parental cells, the expression levels of α-parvin and β-parvin were decreased and concomitant decreases in ILK and PINCH expression were observed. Flow cytometry analysis evaluating the activation state exhibited that the transfection of both α- and β-parvin siRNAs, but not that of either α- or β-parvin siRNA significantly decreased PAC-1 binding (Figure 3D). These data suggest that the IPP complex formation of ILK, PINCH, and parvins is necessary for αIIbα6Bβ3 activation in a CHO cell system.

Knockdown of kindlin-2 in αIIbα6Bβ3-active parental cells

In our previous work, talin siRNA decreased PAC-1 binding to αIIbα6Bβ3-active parental cells [31]. To confirm that kindlin-2 plays an important role in integrin activation in the CHO cell system, we performed the kindlin-2 siRNA experiment in parental cells (Figure 3E, F). Each of two different siRNAs (k770 and k1733) reduced kindlin-2 expression and decreased PAC-1 binding in association without significantly affecting ILK or talin expression. In addition, when an ILK cDNA was cotransfected with kindlin-2 siRNA into ILK-deficient mutant

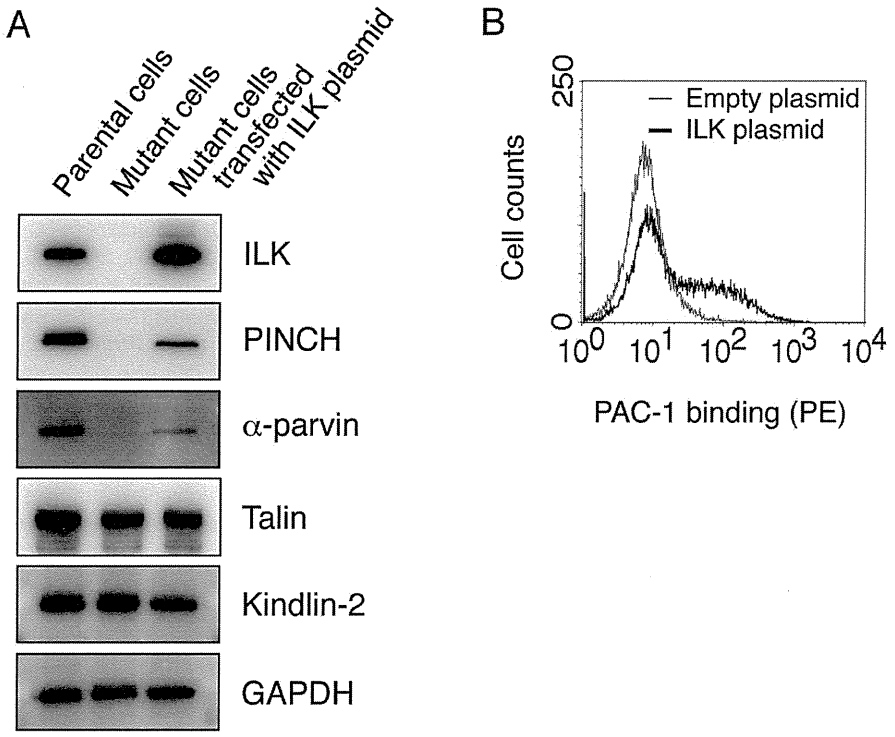

Fig. 1

Figure 1. Characterization of ILK-deficient mutant cells expressing inactive αIIbα6Bβ3. (A) Immunoblotting for ILK, PINCH, α-parvin, talin, and kindlin-2. Cell lysates obtained from parental cells with constitutively active αIIbα6Bβ3, ILK-deficient mutant cells with inactive αIIbα6Bβ3, and mutant cells transiently transfected with rat ILK cDNA were electrophoresed on SDS-PAGE gels and immunoblotted with indicated Abs. GAPDH shows an internal loading control. (B) Flow cytometry analysis showing PAC-1 (an activation-specific mAb for αIIbβ3) binding to mutant cells transiently transfected with either ILK plasmid or empty plasmid. Bound PAC-1 was detected with a PE-conjugated secondary mAb.

doi: 10.1371/journal.pone.0085498.g001

cells, PAC-1 binding was decreased as compared to those of the cotransfection of both the ILK cDNA and scrambled kindlin-2 siRNA (data not shown). These data indicate that kindlin-2 is required for αIIbα6Bβ3 activation in parental cells.

Role in binding of ILK to PINCH and parvin for integrin activation

To examine the significance of ILK-PINCH binding for integrin activation, we generated a GFP-fused ILK mutant (GFPILK-H99D/F109A/W110A) in which mutations were introduced into the binding sites for the LIM1 domain of PINCH in the ankyrin repeat domain of ILK. This ILK mutant is designed to disrupt ILK-PINCH binding but not ILK-α-parvin binding. When GFPILK-WT cDNA was transfected into mutant cells, PAC-1 binding was increased (Figure 4A). Transfection of the GFPILK-H99D/F109A/W110A cDNA into mutant cells failed to recover PAC-1 binding and did not induce an obvious upregulation of PINCH expression, whereas the ILK mutant protein was well expressed and α-parvin was similarly increased compared to the case with GFPILK-WT cDNA transfection, indicating the ILK-α-parvin complex (Figure 4B). These data suggest that ILK-PINCH binding is required for stable PINCH expression even in the presence of ILK, as well as for αIIbα6Bβ3 activation in the CHO cell system. When cell lysates of the mutant cells transfected with the GFPILK-H99D/F109A/W110A cDNA was subjected to immunoprecipitation with anti-α-parvin Ab, the ILK mutant was coprecipitated (data not shown). In addition, we generated a GFP-fused ILK mutant (GFPILK-M402A/K403A) that disrupts the parvin binding and that impairs the localization of ILK to focal adhesions as shown in the previous report [35]. Transfection of GFPILK-M402A/K403A cDNA into mutant cells showed strongly impaired PAC-1 binding and did not induce an overt upregulation of α-parvin expression (Figure 4C, D). These data suggest that ILK-parvin binding is necessary for stable parvin expression, as well as for αIIbα6Bβ3 activation in the CHO cell system.

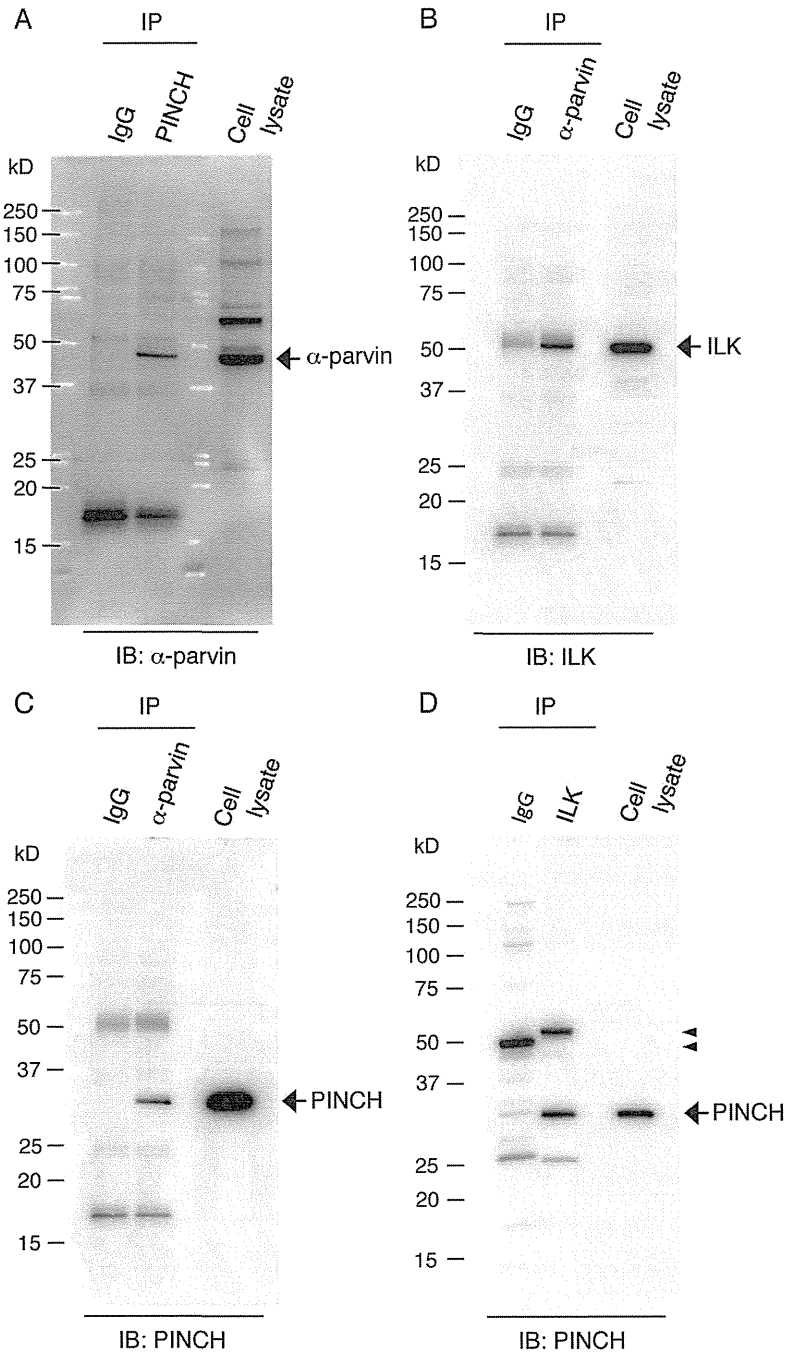

Fig. 2

Figure 2. Detection of IPP complex proteins in αIIbα6Bβ3-active parental cells. Cell lysates obtained from αIIbα6Bβ3-active parental cells were immunoprecipitated with Abs against PINCH (A), α-parvin (B, C), and ILK (D). The co-precipitates were detected by Abs for α-parvin (A), ILK (B), and PINCH (C, D). IgG means immunoprecipitation (IP) using non-immune control IgG. IB stands for immunoblotting. Arrows indicate the predicted sizes of the indicated proteins. Arrowheads (D) indicate the antibody heavy chains used in the IP. Different mobilities between those of the two IgG antibodies are probably caused by differences in the amino acid compositions of them.

doi: 10.1371/journal.pone.0085498.g002

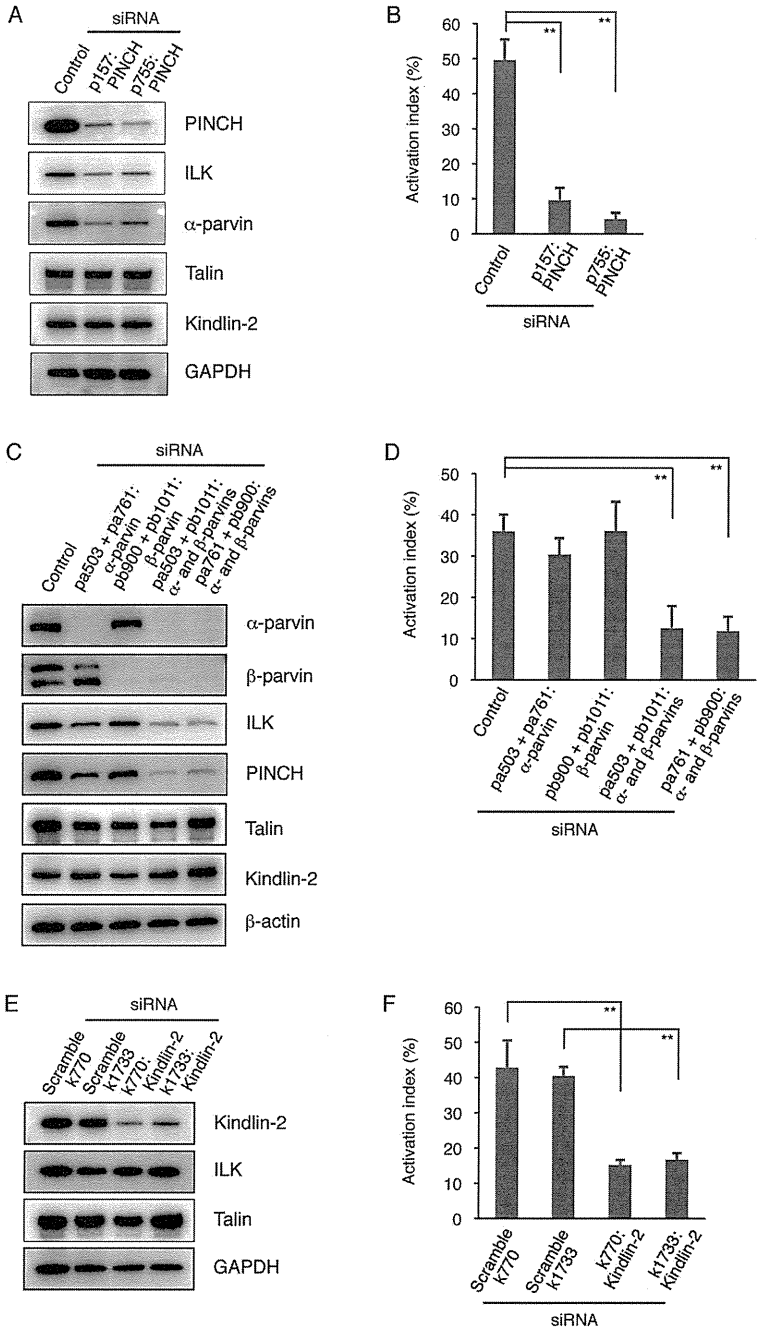

Fig. 3

Figure 3. Knockdown effects of PINCH, parvins, and kindlin-2 in αIIbα6Bβ3-active parental cells. αIIbα6Bβ3-active parental cells were transiently transfected with PINCH siRNAs (p157 and p755) (A), α-parvin siRNAs (pa503 and pa761) (C), β-parvin siRNAs (pb900 and pb1011) (C), kindlin-2 siRNAs (k770 and k1733) (E), negative control siRNAs, and scrambled siRNAs. Cell lysates were electrophoresed on SDS-PAGE gels, and the separated proteins were immunoblotted with the indicated Abs. GAPDH and β-actin are shown as internal loading controls. The activation indexes of transfected cells (B, D, F) were calculated using the formula shown in Materials and Methods. A value of 100% implies the maximum PAC-1 binding to the cells treated with dithiothreitol (DTT). Data represent means ± standard deviation (SD) of three (B, F) or four (D) independent experiments. ** indicates $P < 0.01$.

doi: 10.1371/journal.pone.0085498.g003

Moreover, when fibrinogen, a natural ligand for αIIbβ3, was used instead of PAC-1 in these experiments, similar results were obtained (Figure 4E).

Analysis of ILK in inactive αIIbβ3-expressing CHO cells

αIIbβ3 is present in an inactive state on CHO cells, and overexpression of the THD into those cells can induce αIIbβ3 activation [36]. The THD directly binds the integrin β3 cytoplasmic domain and causes integrin activation. To examine ILK's contribution to THD-mediated αIIbβ3 activation, we performed knockdown experiments targeting ILK under transient THD expression (Figure 5). For the cotransfection of THD-GFP cDNA with scrambled ILK siRNA (scramble Ilk1255), the THD-GFP highly expressing cells exhibited a significant increase in the PAC-1 binding as compared to the case with GFP cDNA cotransfection (Figure 5A, B). In contrast, the cotransfection of THD-GFP cDNA with ILK siRNA (Ilk1255) showed decreased PAC-1 binding in the cells with high expression of THD-GFP (Figure 5A, B). The protein expression levels of ILK, PINCH, and α-parvin were suppressed by the cotransfection of ILK siRNA and THD-GFP cDNA, whereas the expression level of THD-GFP was not changed in the presence of ILK siRNA (Figure 5C). These results suggest that THD is sufficient to restore partially the integrin activation upon elimination of ILK by its siRNA (Ilk1255) and that ILK may assist THD in regulating the integrin activation state by assembling the IPP complex. In addition, these findings obtained from αIIbβ3-expressing CHO cells support the importance of the IPP complex observed in the αIIbα6Bβ3-expressing CHO cells. □

Overexpression of the IPP complex in inactive αIIbβ3-expressing CHO cells

To examine the IPP complex's role in THD-mediated αIIbβ3 activation, we performed overexpression experiments of ILK, PINCH-1, and α-parvin in inactive αIIbβ3-expressing CHO cells. As expected, THD-GFP overexpression into αIIbβ3-expressing CHO cells induced PAC-1 binding in the cells with high expression of THD-GFP, as compared to the case with GFP cDNA transfection (Figure 6A, B). Interestingly, although quadruple overexpression of GFP and IPP did not significantly increase PAC-1 binding, quadruple overexpression of THD-GFP and IPP caused higher PAC-1 binding compared to the case with THD-GFP overexpression, suggesting a supportive effect of IPP on THD-mediated αIIbβ3 activation (Figure 6A, B). Kindlin-2 binds to the integrin β3 cytoplasmic domain and functions as a co-activator of talin [12,37]. As expected, double overexpression of THD-GFP and kindlin-2 cooperatively increased PAC-1 binding (Figure 6A, B), suggesting that both THD and kindlin-2 are required for the full activation of αIIbβ3. Regarding protein expression, THD-GFP was adequately expressed in each transfection, and the expression levels of ILK, PINCH, α-parvin, and kindlin-2 were higher than their endogenous expression levels in the cells with indicated transfection (Figure 6C). Thus, these data suggest that the IPP complex supports the THD for integrin αIIbβ3 activation.

Discussion

ILK is a multidomain scaffold protein that interacts with several cytoplasmic proteins [38,39]. In integrin adhesion sites, ILK exists in a ternary complex composed of the two other proteins PINCH and parvin. The ternary complex formation can stabilize each component and exert its function. In fact, ILK-deficient mutant CHO cells exhibited profoundly reduced PINCH and α-parvin expression levels, leading to inactive αIIbα6Bβ3 (Figure 1). The introduction of ILK expression into ILK-deficient mutant cells increased the expression levels of PINCH and α-parvin, accompanied by αIIbα6Bβ3 activation (Figure 1). The involvement of the IPP complex formation in integrin activation was confirmed in the knockdown experiments of PINCH and parvins in αIIbα6Bβ3-active parental cells (Figure 3). The ILK mutants with defects in either PINCH or parvin binding did not activate αIIbα6Bβ3 in ILK-deficient mutant cells (Figure 4). Since it has been reported that the parvin-binding defective ILK mutant (M402A/K403A) fails to localize to focal adhesions [35], these two ILK mutants are probably not recruited to the αIIbα6Bβ3 sites in a process of integrin activation. Thus, our data support a previous report that the proper complex formation of ILK, PINCH, and parvin is necessary for ILK recruitment to the integrin adhesion sites [35,40].

Recent studies of integrin regulatory proteins have shown that both talin and kindlins directly bind to different regions in the integrin β cytoplasmic domain and cooperate in a final step of integrin activation [9,12]. In our experiments, kindlin-2 knockdown in αIIbα6Bβ3-active parental cells reduced the activation state of αIIbα6Bβ3, and talin knockdown exhibited similar results in our previous work [31]. The knockdown of PINCH and of parvins in the IPP complex decreased the activation state of αIIbα6Bβ3 in parental cells to a similar extent as did the knockdown of either kindlin-2 or talin. In inactive αIIbβ3-expressing CHO cells, overexpression of THD-GFP induced αIIbβ3 activation, and ILK knockdown reduced THD-GFP-mediated αIIbβ3 activation (Figure 5). Moreover, overexpression of the IPP complex further augmented the activation state of αIIbβ3 induced by the THD in inactive αIIbβ3-expressing CHO cells (Figure 6). These data suggest that the IPP complex participates in the cooperation of talin and kindlin-2 during the activation processes of not only αIIbα6Bβ3 but also αIIbβ3. The precise binding sites of ILK in the integrin β cytoplasmic domain remain to be determined, although their interaction has been reported [19]. There seem to be two possible direct and indirect manners of ILK binding to the integrin cytoplasmic domain. It was recently reported that the binding of PAT-4 (ILK) to UNC-112 (kindlin) in *C. elegans* is necessary for UNC-112 recruitment to adhesion sites [41]. While kindlin alone appears to bind to integrin in mammalian cells, the IPP complex would contribute to effective binding of kindlin to the β integrin cytoplasmic domain to fully induce conformational changes of integrin.

Adaptor proteins, PINCH-1 and -2, share high amino acid sequence identity [27]. Those are ubiquitously expressed in different tissues and show overlapping expression in many tissues. Both isoforms bind equally well to ILK, but its binding is

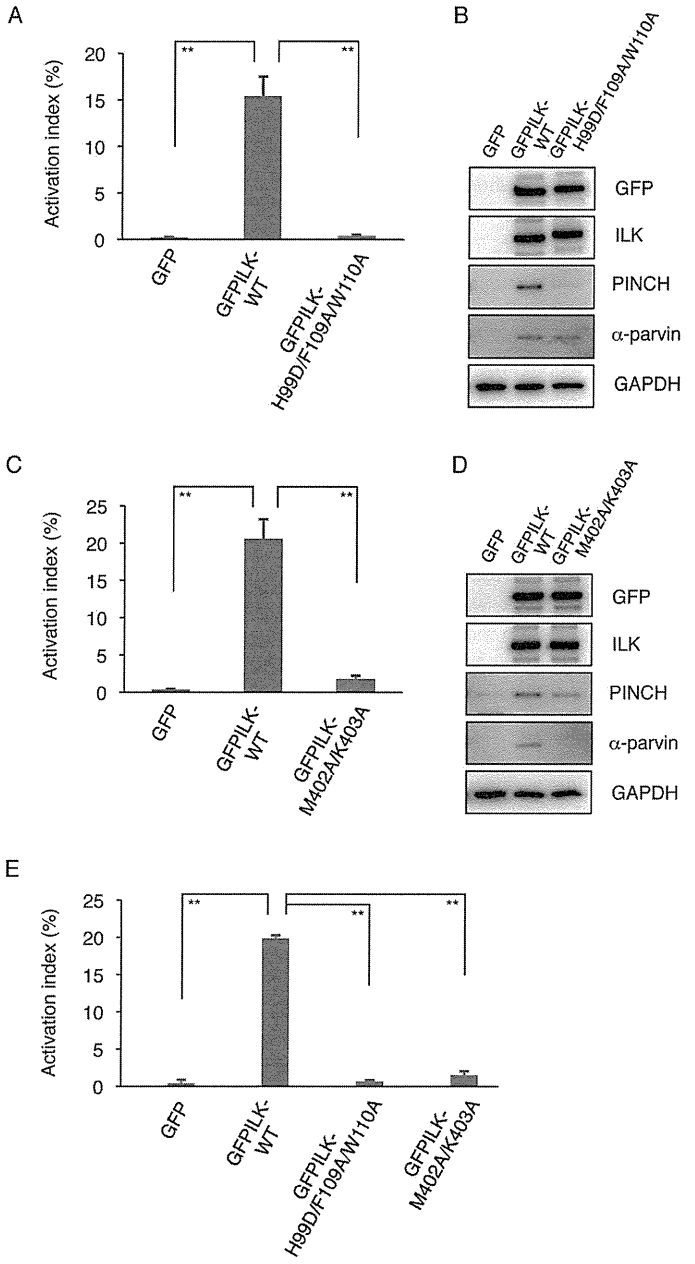

Fig.4

Figure 4. Effects of ILK mutants with defects in either PINCH or parvin binding. The activation indexes of transfected cells (A, C, E). ILK-deficient mutant cells were transiently transfected with GFP cDNA, GFP-fused wild-type ILK (GFPILK-WT) cDNA, GFP-fused ILK mutant with defective PINCH binding (GFPILK-H99D/F109A/W110A) cDNA (A, E), or GFP-fused ILK mutant with defective parvin binding (GFPILK-M402A/K403A) cDNA (C, E). After transfection, the binding of either PAC-1 (A, C) or fibrinogen (E) to the cells was analyzed by flow cytometry. The activation index was determined by the formula shown in Materials and Methods. A value of 100% represents the maximal binding of PAC-1 or fibrinogen to the cells treated with dithiothreitol. Data represent means ± SD of three independent experiments. ** indicates $P < 0.01$. Immunoblotting showing protein expression of GFP (B, D), GFP-fused wild-type ILK (GFPILK-WT) (B, D), GFP-fused ILK mutant with defective PINCH binding (GFPILK-H99D/F109A/W110A) (B), and GFP-fused ILK mutant with defective parvin binding (GFPILK-M402A/K403A) (D) in ILK-deficient mutant cells. Cell lysates were electrophoresed and immunoblotted with indicated Abs.

doi: 10.1371/journal.pone.0085498.g004